Resource

Cell Stem Cell

Efficient Detection and Purification of Cell Populations Using Synthetic MicroRNA Switches

Graphical Abstract

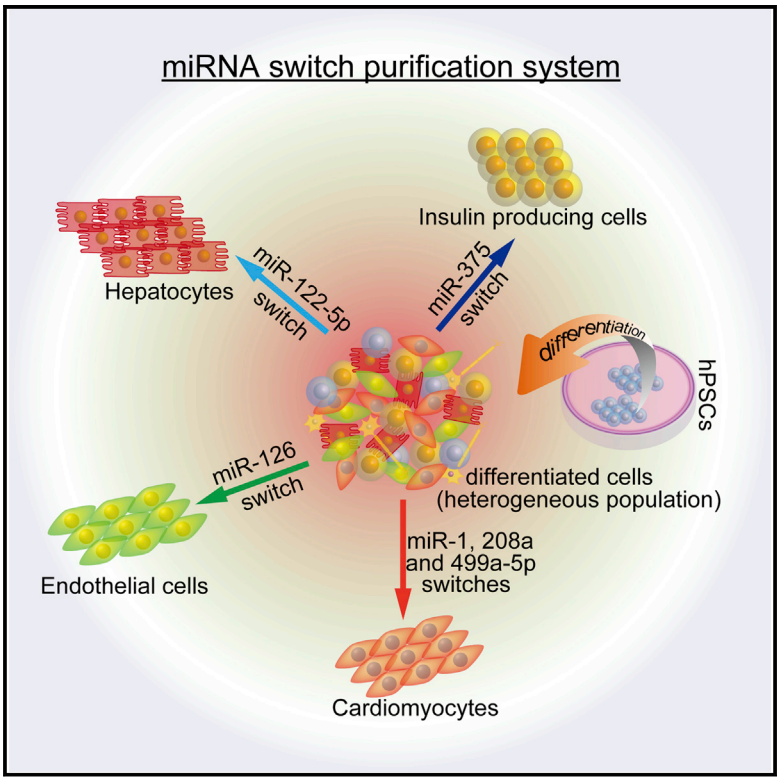

Highlights

- Synthetic miRNA switches can purify target cell populations based on miRNA activity
- miR-1-, -208a-, and -499a-5p-switches highly purify hPSC-derived cardiomyocytes
- miR-Bim switches enrich for cardiomyocytes without the need for cell sorting
- miRNA switches can isolate desired cell types without significant side effects

Authors

Kenji Miki, Kei Endo, ..., Hirohide Saito, Yoshinori Yoshida

Correspondence

hirohide.saito@cira.kyoto-u.ac.jp (H.S.), yoshinor@cira.kyoto-u.ac.jp (Y.Y.)

In Brief

Miki et al. develop synthetic miRNA switches for isolating cell populations that are otherwise difficult to purify. Several miRNA-responsive switches precisely and efficiently isolate human pluripotent stem cell (hPSC)-derived cardiomyocytes, and miRNA switches can be programmed for purification of various cell types including hPSC-derived endothelial cells, hepatocytes, and insulin-producing cells.

Accession Numbers

GSE60633

Miki et al., 2015, Cell Stem Cell *16*, 1–13
June 4, 2015
http://dx.doi.org/10.1016/j.stem.2015.04.005

CellPress

Please cite this article in press as: Miki et al., Efficient Detection and Purification of Cell Populations Using Synthetic MicroRNA Switches, Cell Stem Cell (2015), http://dx.doi.org/10.1016/j.stem.2015.04.005

Cell Stem Cell
Resource

Efficient Detection and Purification of Cell Populations Using Synthetic MicroRNA Switches

Kenji Miki,[1,2,7] Kei Endo,[1,3,7] Seiya Takahashi,[1] Shunsuke Funakoshi,[1,4] Ikue Takei,[1] Shota Katayama,[1] Taro Toyoda,[1] Maki Kotaka,[1] Tadashi Takaki,[1] Masayuki Umeda,[1,5] Chikako Okubo,[1] Misato Nishikawa,[1] Akiko Oishi,[1] Megumi Narita,[1] Ito Miyashita,[1] Kanako Asano,[1] Karin Hayashi,[1] Kenji Osafune,[1] Shinya Yamanaka,[1,2,6] Hirohide Saito,[1,*] and Yoshinori Yoshida[1,*]

[1]Center for iPS Cell Research and Application, Kyoto University, Kyoto, 606-8507, Japan
[2]Institute for Integrated Cell-Material Sciences (WPI-iCeMS), Kyoto University, Kyoto 606-8507, Japan
[3]Department of Medical Genome Sciences, Graduate School of Frontier Sciences, The University of Tokyo, Kashiwa-shi, Chiba, 277-8562, Japan
[4]Department of Cardiovascular Medicine, Graduate School of Medicine, Kyoto University, Kyoto, 606-8507, Japan
[5]Department of Hematology and Oncology, Graduate School of Medicine, Kyoto University, Kyoto, 606-8507, Japan
[6]Gladstone Institute of Cardiovascular Disease, San Francisco, CA 94158, USA
[7]Co-first author
*Correspondence: hirohide.saito@cira.kyoto-u.ac.jp (H.S.), yoshinor@cira.kyoto-u.ac.jp (Y.Y.)
http://dx.doi.org/10.1016/j.stem.2015.04.005

SUMMARY

Isolation of specific cell types, including pluripotent stem cell (PSC)-derived populations, is frequently accomplished using cell surface antigens expressed by the cells of interest. However, specific antigens for many cell types have not been identified, making their isolation difficult. Here, we describe an efficient method for purifying cells based on endogenous miRNA activity. We designed synthetic mRNAs encoding a fluorescent protein tagged with sequences targeted by miRNAs expressed by the cells of interest. These miRNA switches control their translation levels by sensing miRNA activities. Several miRNA switches (miR-1-, miR-208a-, and miR-499a-5p-switches) efficiently purified cardiomyocytes differentiated from human PSCs, and switches encoding the apoptosis inducer Bim enriched for cardiomyocytes without cell sorting. This approach is generally applicable, as miR-126-, miR-122-5p-, and miR-375-switches purified endothelial cells, hepatocytes, and insulin-producing cells differentiated from hPSCs, respectively. Thus, miRNA switches can purify cell populations for which other isolation strategies are unavailable.

INTRODUCTION

Cardiovascular disease is the most common cause of death worldwide. Many therapeutic strategies to treat cardiovascular disease are being investigated, including human pluripotent stem cells (hPSCs), such as embryonic stem cells (hESCs) and induced pluripotent stem cells (hiPSCs), which can produce a variety of cell types and which are a potential cell source for transplantation therapy, drug efficiency evaluation, and toxicology testing (Garbern and Lee, 2013; Takahashi et al., 2007; Yu et al., 2007). In particular, the transplantation of cardiomyocytes derived from hPSCs is a promising strategy for reconstructing damaged myocardium.

Although several studies on the differentiation of hPSCs into cardiomyocytes have been reported (Kawamura et al., 2013; Laflamme et al., 2007; Li et al., 2011; White et al., 2013; Yang et al., 2008), the resulting differentiated cells are often a mixture of heterogeneous populations. Therefore, the purification of distinct target cells, such as cardiomyocytes, is an important step for safe and controllable cell therapy. However, many types of cells, including cardiomyocytes, have no specific cell surface markers that facilitate their identification, thus hindering the clinical applications of hPSC-derived cells.

To overcome this problem, several methods have been devised for purifying hPSC-derived cardiomyocytes. Examples include a Percoll density gradient procedure (Laflamme et al., 2007; Xu et al., 2002); genetic manipulation of hPSCs using cardiac promoters (Anderson et al., 2007; Bizy et al., 2013; Elliott et al., 2011); cell sorting using mitochondrial dyes (Hattori et al., 2010), molecular beacons that target cardiomyocyte-specific mRNA (Ban et al., 2013) or antibodies against cardiac cell surface markers, including signal-regulatory protein alpha (SIRPA) (Dubois et al., 2011) and vascular cell adhesion molecule 1 (VCAM1) (Elliott et al., 2011; Uosaki et al., 2011); and metabolic selection using glucose-depleted culture medium containing lactate (Tohyama et al., 2013). Some of these methods, such as those that require genetic modification, are likely inappropriate for transplantation therapy. Although cell sorting using antibodies should initially enable enrichment of cardiomyocytes, markers such as SIRPA and VCAM1 are expressed in other cell types (Dubois et al., 2011; Osborn et al., 1989). This potential non-specificity could cause contamination by non-cardiomyocytes, affecting the efficacy of the transplantation. Moreover, antibodies on the surface of transplanted cells may be immunogenic and cause local inflammation or graft failure. Therefore, we investigated an alternative purification method that is based on detecting and distinguishing

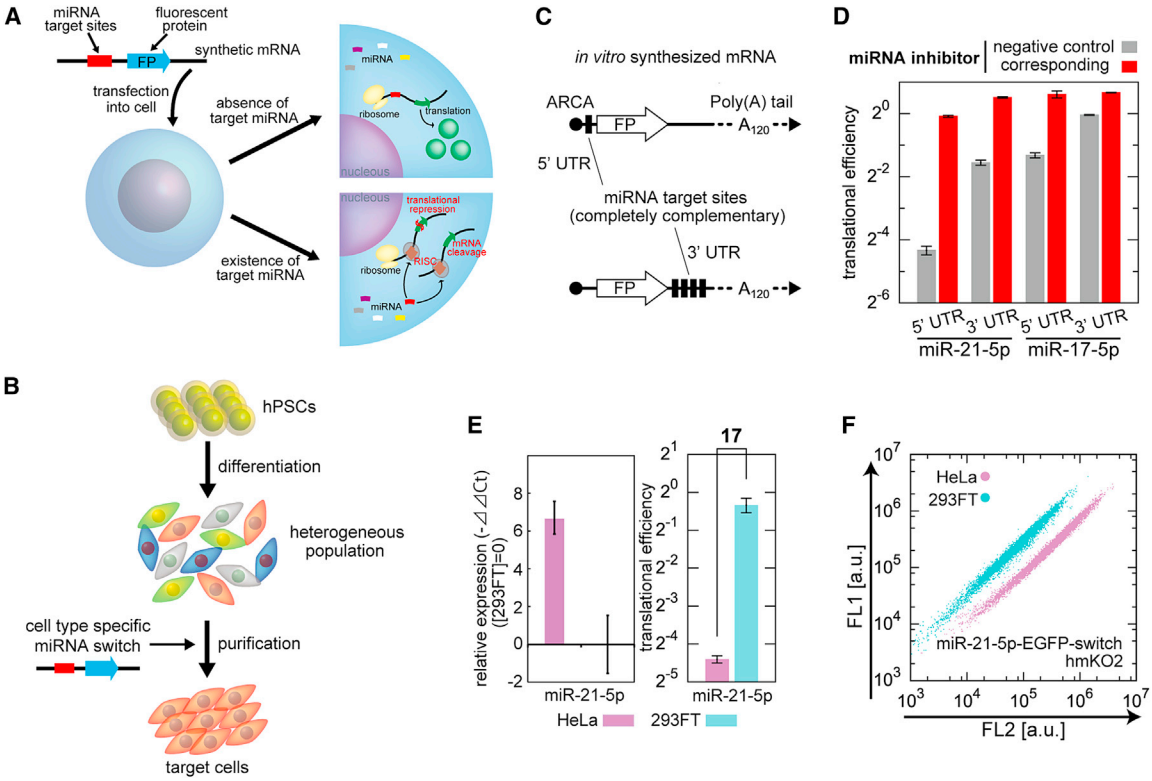

Figure 1. Measurement of miRNA Activity Using miRNA Switches

(A) Schematic representation of miRNA switch function.

(B) Scheme of target cell purification using a cell-type-specific miRNA switch.

(C) Design of a miRNA switch synthesized in vitro. The upper and lower constructs contain one miRNA target site in the 5′ UTR and four sites in the 3′ UTR, respectively, as well as a fluorescent protein coding sequence. Each target site was completely complementary to the miRNA of interest. Synthesized mRNAs contain anti-reverse cap analog (ARCA) at the 5′ end and a poly(A) tail of 120 nucleotides (A120).

(D) Translational efficiency of the designed mRNAs measured in the presence of a miRNA inhibitor. Reporter mRNAs expressing EGFP and the control tagRFP mRNA were transfected into HeLa cells together with a miRNA inhibitor. The inhibitor was responsive to miR-21-5p or miR-17-5p (corresponding, red) or to miR-1 (negative control, gray). Translational efficiency was defined as the mean intensity of EGFP divided by that of tagRFP, followed by normalization with control EGFP mRNA. The error bars indicate the mean ± SD (n = 5).

(E) Left, analysis of endogenous miR-21-5p expression by qRT-PCR. The error bars indicate the geometric mean ± SD from two independent triplicates. Right, translational efficiency of miR-21-5p-EGFP-switch in HeLa and 293FT cells. The fold change is shown at the top. The error bars indicate the mean ± SD (n = 3).

(F) Dot plots of HeLa (magenta) and 293FT (cyan) cells. The cells were transfected with miR-21-5p-EGFP-switch (FL1) and control hmKO2 mRNA (FL2) and analyzed by flow cytometry 24 hr later.

microRNA (miRNA) activities in living target cells from non-target cells.

miRNAs are small non-coding RNAs that downregulate gene expression by translational repression or mRNA cleavage (Figure 1A). Recent progress in synthetic biology approaches (Khalil and Collins, 2010; Ye et al., 2013; Zhang and Seelig, 2011) has demonstrated that DNA-based genetic circuits can control gene expression depending on miRNA activities (Leisner et al., 2010; Rinaudo et al., 2007; Xie et al., 2011). However, DNA-based circuits have the potential risk of genome incorporation. To avoid potential genomic damage, modified mRNAs (modRNAs) have been used to reprogram human somatic cells into hPSCs (Warren et al., 2010). The in vivo injection of a modRNA into an ischemic heart also improved cardiac function and long-term survival (Zangi et al., 2013).

We hypothesized that the use of a miRNA-responsive, synthetic modRNA switch (miRNA switch) could enable better purification of desired cell types differentiated from hPSCs in terms of efficiency, selectivity, and safety (Figures 1A and 1B). The miRNA switches were designed such that their translation level was dependent on the target miRNA activity. We also found that the selective induction of apoptosis in non-target cells triggered by the miR-Bim-switch autonomously purified cardiomyocytes without cell sorting, a process that may damage cells. Furthermore, the corresponding miRNA switches efficiently purified endothelial cells, hepatocytes and INSULIN-producing cells differentiated from hPSCs. Thus, this miRNA switch technology could be useful to purify desired cell types for future therapeutic applications and regenerative medicine.

RESULTS

Design and Evaluation of miRNA Switches in HeLa Cells

We first designed and evaluated the function of miRNA switches in cells from the human HeLa cell line. We initially designed two reporter mRNAs that contained a miRNA target sequence that is completely complementary to the miRNA at either the 5′ UTR or the 3′ UTR based on miRBase 19 (Kozomara and Griffiths-Jones, 2011). The antisense sequence for a particular miRNA was present as either a single copy or four copies in the 5′ UTR or 3′ UTR of the mRNA, respectively (Figure 1C). To compare the sensitivities in detecting the activity of endogenous miRNA for these two miRNA switch types, we designed both types to be responsive to miR-21-5p and miR-17-5p (both of which are active in HeLa cells) and transfected each mRNA into the cells (Figure 1D). In the absence of an inhibitor for the particular miRNA, the translation efficiency of the reporter EGFP was lower when the antisense sequence was incorporated upstream (5′ UTR) of the ORF than downstream (3′ UTR) of the ORF (Figure 1D, gray bars). The EGFP production level was readily recovered in the presence of the corresponding inhibitor (Figure 1D, red bars). These results indicate that transferred mRNA with a single target site in the 5′ UTR can respond to endogenous miRNAs and repress translation more effectively. Thus, we inserted a single miRNA target site in the 5′ UTR of reporter mRNA and used this product as a platform to design the miRNA switch.

We investigated whether the designed miRNA switch could distinguish the HeLa cells from 293FT cells. Using EGFP-mRNA that responds to miR-21-5p (miR-21-5p-EGFP-switch), we compared the translational repression efficiency between HeLa and 293FT cells. The measured translational efficiency in HeLa cells was 17-fold lower than that in 293FT cells, indicating higher miR-21-5p activity in HeLa cells than in 293FT cells (Figure 1E, right). We performed qRT-PCR analysis and confirmed that the expression level of endogenous miR-21-5p in HeLa cells was higher than that in 293FT cells (Figure 1E, left). Next, we co-transfected both miR-21-5p-EGFP-switch and the control, i.e., humanized monomeric Kusabira-Orange 2 mRNA (hmKO2). Interestingly, we observed clearly separated HeLa and 293FT cell populations that were co-transfected with these two mRNAs (Figure 1F). The dot plot shows specific and sharp bands of two cell types in which one reporter fluorescent signal (EGFP or FL1) was in direct proportion to the other (hmKO2 or FL2). This result indicates that the ratio of the two fluorescent proteins translated from the two mRNAs is almost constant in the population of one cell type and is determined by miRNA activity, regardless of the amount of modRNA that each cell receives. This demonstrates that HeLa cells can be identified and separated from 293FT cells using our synthetic miRNA switch approach.

Screening for Cardiac-Specific miRNA Candidates

We next investigated whether the designed miRNA switch could be used to identify and purify hPSC-derived cardiomyocytes. We screened for cardiac-specific miRNAs using a hiPSC line into which a human MYH6 promoter driven-EGFP reporter cassette was integrated (MYH6-EIP4) (S.F., K.M., T.T., C.O., T. Hatani, K. Chonabayashi, M.N., I.T., A.O., M.N., T. Kimura., S.Y., and Y.Y., unpublished data). MYH6-EIP4 hiPSCs were differentiated into cardiomyocytes using the appropriate concentrations of Activin A and BMP4 (see Supplemental Experimental Procedures). EGFP-positive (EGFP$^+$) cells appeared from day 8 (Figure S1A), and most of the sorted EGFP$^+$ cells at day 8 and day 20 expressed the cardiac isoform of Troponin T (cTNT), a cardiomyocyte-specific marker (Figure S1B).

To select for cardiomyocyte-specific miRNA candidates, we compared the expression profiles of miRNA between EGFP$^+$ cardiomyocytes and EGFP$^-$ non-cardiomyocytes derived from the MYH6-EIP4 iPSC line at day 8 and day 20. We identified differentially expressed miRNAs at day 8 (28 candidates) and day 20 (81 candidates; fold change >4). Among them, 14 miRNAs were shared between the day 8 and day 20 differentially expressed miRNA groups (Figures 2A–2C). Accordingly, we synthesized 14 miRNA switches that included the sequence of blue fluorescent protein (BFP) as a reporter (miR-BFP-switch). To evaluate the function of these miR-BFP switches, we individually transfected the switches with control EGFP mRNA into differentiated cells, including hiPSC-derived cardiomyocytes (201B7 cell line (Takahashi et al., 2007), day 19 of differentiation). Interestingly, we found that BFP signals translated from three miRNA (miR-1, miR-208a, and miR-499a-5p) switches clearly separated the cells into two populations within a heterogeneous starting population (Figure 2D), whereas the signal from control BFP mRNA did not, indicating that miR-1-, miR-208a-, and miR-499a-5p-switches repressed BFP translation by interacting with the corresponding miRNAs expressed in the cardiomyocytes. Additionally, miR-143-3p-, miR-490-3p-, and miR-490-5p-switches did not clearly separate the cells into two subpopulations. The other eight miRNA switches did not significantly repress BFP signals compared with control BFP mRNA. Thus, we focused on miR-1-, miR-208a-, and miR-499a-5p-switches as candidates for the purification of cardiomyocytes.

Purification of hPSC-Derived Cardiomyocytes

To investigate whether miRNA switches could purify hPSC-derived cardiomyocytes, we collected separated cells with repressed BFP signals (gated cells are enclosed by the red solid line in Figure 2D) by cell sorting on day 20 and analyzed cTNT expression by flow cytometric analysis (Figure S2A). Most of the sorted cells with miR-1-, miR-208a- and miR-499a-5p-switches were cTNT-positive cells (cTNT$^+$; miR-1, 95.73% ± 1.44%; miR-208a, 96.17% ± 1.29%; miR-499a-5p, 95.5% ± 2.28%), whereas those cells sorted with miR-143-3p-switch showed a lower percentage of cTNT$^+$ cells (30.07% ± 10.57%), similar to cells sorted with the deficient miR-490-3p-switch (27.40% ± 9.32%) and to control cells without sorting (24.43% ± 2.16%; Figure 3A and Figure S2A). To compare the purification efficiencies with existing methods, we purified cardiomyocytes from 201B7-derived differentiated cells on day 20 using the cardiac-specific surface marker SIRPA$^+$ LIN$^-$ (CD31, CD49a, CD90, and CD140b) (Dubois et al., 2011) or VCAM1$^+$ (Uosaki et al., 2011) (Figures S2B and S2C). The percentages of cTNT$^+$ cardiomyocytes in SIRPA$^+$ LIN$^-$ and VCAM1$^+$ cells were 75.27% ± 13.09% and 49.33% ± 4.76%, respectively, indicating that miRNA switches can purify cTNT$^+$ cells more efficiently (Figure 3A). We also compared the false negative rate of the isolation method by sorting the unreacted cells using either miRNA switches or antibodies (SIRPA and VCAM1) to collect a non-targeted cell population (negative fraction). The proportions

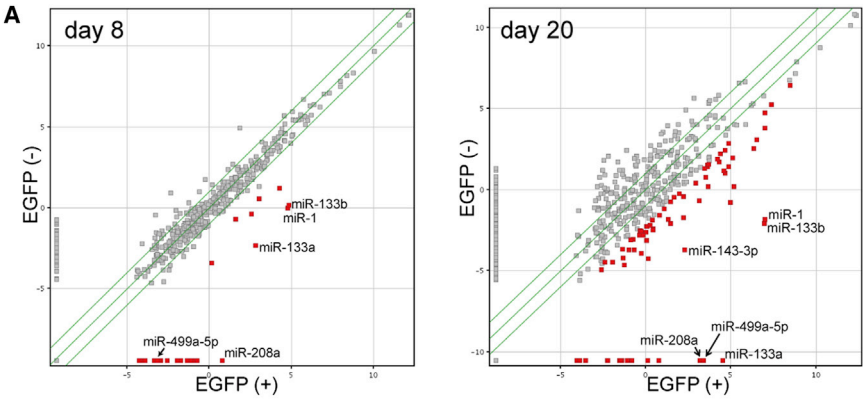

Figure 2. Identification of Cardiac-Specific miRNA in hiPSC-Derived Cardiomyocytes

(A) Scatter plot of MYH6-EIP4-derived EGFP$^+$ and EGFP$^-$ cells on day 8 and day 20. The red dots are candidate miRNAs significantly expressed in EGFP$^+$ cells compared with EGFP$^-$ cells (fold change >4).

(B) Venn diagram of day 20 and day 8 candidates.

(C) List of cardiac-specific miRNA candidates.

(D) Flow cytometric analysis of candidate miRNA switches using 201B7-derived differentiated cells. Solid and dashed red lines represent repressed and non-repressed BFP signals, respectively.

See also Figure S1.

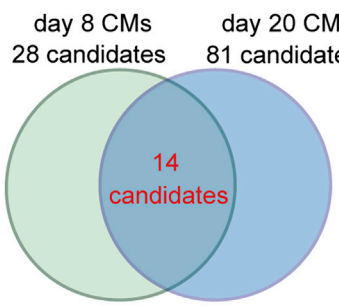

C

14 candidates list

hsa-miR-1	hsa-miR-490-3p
hsa-miR-22-5p	hsa-miR-490-5p
hsa-miR-133a	hsa-miR-499a-5p
hsa-miR-133b	hsa-miR-1271-5p
hsa-miR-143-3p	hsa-miR-3907
hsa-miR-145-3p	hsa-miR-4324
hsa-miR-208a	hsa-let-7e-5p

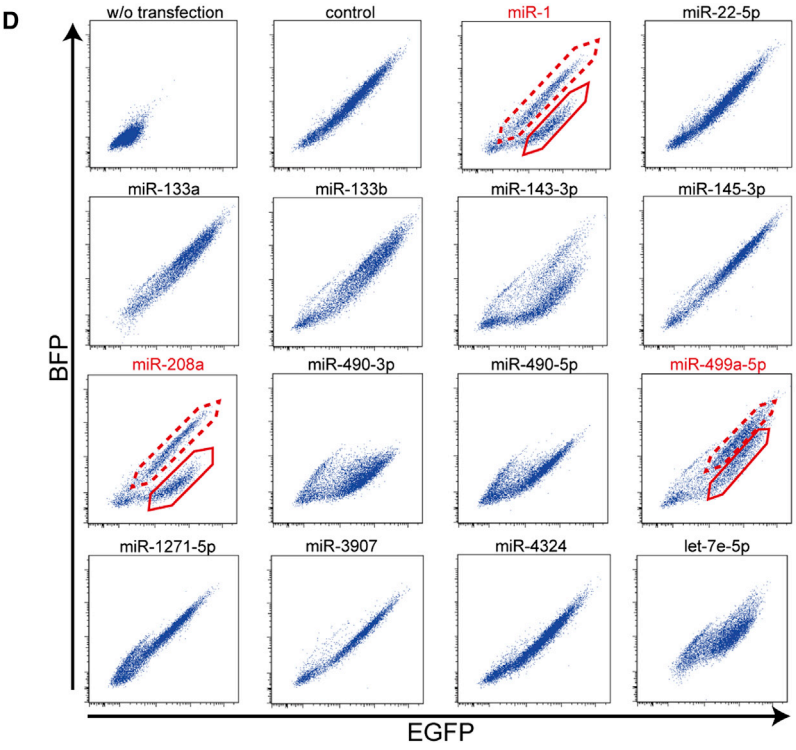

of cTNT$^+$ cardiomyocytes in the negative fraction were 7.95% ± 2.24% (miR-1), 8.85% ± 5.10% (miR-208), 17.96% ± 10.99% (miR-499a-5p), 11.40% ± 6.32% (SIRPA$^+$ LIN$^-$), and 21.25% ± 6.76% (VCAM1$^+$). In the case of miRNA switches, most of cTNT$^+$ cells in the negative fraction showed no EGFP expression, indicating that these cTNT$^+$ cells were mRNA non-transfected cells (Figure S2D). In addition, hierarchical clustering of the cells sorted by these purification methods demonstrated that the gene expression profiles of miR-208a-switch-sorted cells are similar to MYH-EIP4 EGFP$^+$- or the antibody-sorted cells (Figure S2E). These results verified that the miRNA switches isolated cTNT$^+$ cardiomyocytes with high accuracy and efficiency.

To investigate whether the three miRNA switches could detect and purify cardiomyocytes derived from other hPSC lines, we analyzed differentiated cells from three different hiPSC lines (409B2, 606A1, and 947A2) and from one hESC line (KhES1). We analyzed the percentages of cTNT$^+$ cells after sorting the differentiated cells from each of the four hPSC lines using the following three purification approaches: repressed and unrepressed (negative fraction) BFP signals in the miRNA switch-transfected cells, the SIRPA$^+$ LIN$^-$ cells, and the VCAM1$^+$ cells. All three miRNA switches showed high purification efficiencies (more than 95%) for all four hPSC lines (Figure 3B and Table S1), whereas the proportion of cTNT$^+$ cells sorted by SIRPA$^+$ LIN$^-$ or VCAM1$^+$ cells ranged between 60% and 85%. Immunocytochemistry of the cardiomyocytes purified using miR-1-, miR-208a-, and miR-499a-5p-switches confirmed that most of the sorted cells were positive for cTNT (Figure 3C, top), while the cells in each negative fraction contained a small number of cTNT$^+$ cells (Figure 3C, bottom), most of which were considered non-transfected cells. These results indicate that the miRNA switches have high efficiency and robustness for the purification of cardiomyocytes.

To further determine whether miR-1-, miR-208a-, and miR-499a-5p-switches isolate cardiomyocytes during the early phase of cardiomyocyte differentiation, we transfected the miRNA switches into differentiated cells on day 8 instead of day 20, and the cTNT analysis was performed 1 day later (day 9). The miR-208a-switch efficiently purified cTNT$^+$ cardiomyocytes (>95%), whereas miR-1-switch had poor separation and sorting purity (Figure 3D and Figure S3A). miR-499a-5p-switch did not react to day 8 differentiated cells (Figure S3A). When sorting SIRPA$^+$ LIN$^-$ cells at day 9, cTNT$^+$ cardiomyocytes were modestly enriched in a manner similar to miR-1-switch sorting, and VCAM1$^+$ cells were not detected in day 9 differentiated cells (Figure 3D and Figure S3A). Taken together, miR-208a-switch had the best performance, isolating even primitive cTNT$^+$ cardiomyocytes with high accuracy.

Functional Evaluation of Cardiomyocytes Purified by miR-1-Switch

As a representative miRNA switch to purify cardiomyocytes, we further focused on the effect of miR-1-switch and evaluated the corresponding purified cardiomyocytes. We analyzed the gene expression levels and electrophysiological state of the miR-1-switch-sorted cells. qRT-PCR analysis demonstrated that the sorted cells showed significantly higher expression of cardiac markers (MYH6, MYH7, MYL2, MYL7, TNNT2, NKX2.5, and TBX5) and lower expression of non-cardiomyocyte markers (PECAM1, THY1, and PDGFR-beta) compared with negative fraction cells and unsorted cells (Figure S3B). In addition, action potential recordings detected both ventricular-like and atrial-like waveforms in the purified cardiomyocytes (Figure S3C).

To assess any possible side effects of the reporter mRNA and miR-1-switch transfection on cardiomyocytes, we analyzed residual levels of the mRNA and protein in EGFP$^+$ cardiomyocytes derived from MYH6-EIP4 hiPSCs. After the transfection of BFP mRNA, the expression level of BFP proteins from modRNA reached a plateau between 12-24 hr and decreased to near background levels in 7 days (Figure 3E). We also analyzed residual EGFP mRNA levels in miR-1-switch-sorted cardiomyocytes derived from 201B7 cells using qRT-PCR and found that transfected mRNAs were immediately degraded within 48 hr (Figure 3F). Next, we investigated whether the transfected miR-1-switch (miR-208a- and miR-499a-5p-switches) could deplete the endogenous miR-1 (miR-208a and miR-499a-5p) in MYH6-EGFP-sorted cardiomyocytes. qRT-PCR analysis revealed that the total amount of endogenous miR-1 (miR-208a and miR-499a-5p) underwent only minimal changes between cardiomyocytes before and 24 hr after transfection (Figure 3G) and between cardiomyocytes with and without transfection of the corresponding switches (Figures 3G and S3D). In addition, we investigated whether miR-1-switch transfection affected global gene expression patterns, including those of miR-1 target genes. We performed microarray analysis, and the hierarchical clustering of all genes and miR-1-target genes revealed that the expression profiles of miR-1-switch-transfected cells were similar to non-transfected cells at both one day (day 19) and 7 days (day 25) after transfection (Figure 3H). Moreover, qRT-PCR analysis of GATA4 and HAND2, which are known target cardiac genes of miR-1, showed that no significant differences were observed between transfected and non-transfected cells at 24 hr and 72 hr after transfection (Figure S3E). Therefore, miR-1-switch had no significant side effects and maintained normal gene expression profiles in cardiomyocytes.

Selective Apoptosis Control and Cardiomyocyte Purification without Cell Sorting

One of the merits when using miRNA switches is the versatility of the ORF used in the mRNA sequence. For example, we could incorporate a desired transgene into the miRNA switches to control the cell phenotype based on miRNA activity. Thus, we investigated whether miR-Bim-switch, which regulates selective cell death, could be employed to concentrate cardiomyocytes from heterogeneous cell populations without cell sorting. Both miR-1- and miR-208a-Bim-switches were constructed; these switches were designed to induce apoptosis selectively in cells other than cardiomyocytes (Figure 4A). To select for the transfected cells, we simultaneously transfected puromycin resistance mRNA (puro^r-mRNA), which triggered the death of non-transfected cells when culturing in the presence of puromycin (Figure 4A). First, we optimized the concentrations of puromycin and puro^r-mRNA (Figures S4A and S4B) and then transfected miR-1- or miR-208-switches with puro^r-mRNA into hPSC-derived cells. Importantly, miR-1- and miR-208a-Bim-switches enabled the highly specific purification of cTNT$^+$ cardiomyocytes without cell sorting (Figure 4B). Immunohistochemical analysis confirmed that almost all of the surviving cells expressed cTNT proteins (Figure 4C). The recovered proportions of 201B7-, 409B2-, and KhES1-derived cardiomyocytes under 75 ng/ml miR-208a-Bim conditions were 90.0% ± 7.9%, 90.5% ± 2.5%, and 89.0% ± 4.1%, respectively (Figure 4D). These recovery yields were higher than the transfection efficiency (Figure 3E) probably because of the efficient proliferation of the surviving cardiomyocytes. Activating cell death by Bim induction may have potentially harmful side effects on the surviving cardiomyocytes. We therefore investigated the hierarchical clustering of cell death pathway-related genes and revealed that the expression profiles of miR-208a-Bim-switch-transfected cardiomyocytes were similar to non-transfected cardiomyocytes at one day (day 19), 3 days (day 21), and 7 days (day 25) after transfection, indicating negligible harmful side effects of miR-Bim-switch transfection on the surviving cardiomyocytes (Figure S4C). Taken together, our miR-Bim-switch system is a highly efficient and safe purification method for cardiomyocytes without the need for cell sorting.

Transplantation of Cardiomyocytes Purified by miRNA Switch

To demonstrate whether this technology is applicable for cardiomyocyte transplantation therapy, we transplanted miR-208a-Bim-switch-purified cardiomyocytes into the hearts of non-obese diabetic/severe combined immunodeficiency interleukin-2 receptor γ^{null} (NOD/Shi-scid Il2rg^{null}; NOG) mice with acute myocardial infarction. In this experiment, we used a luciferase reporter-expressing hiPSC line to detect the 1×10^6 cardiomyocytes that were purified by miR-208a-Bim-switch and transplanted into the heart. We detected the luciferase signal for more than 3 months (Figure 5A). Immunostaining demonstrated that transplanted cells (human nuclei [hN]-positive cells)

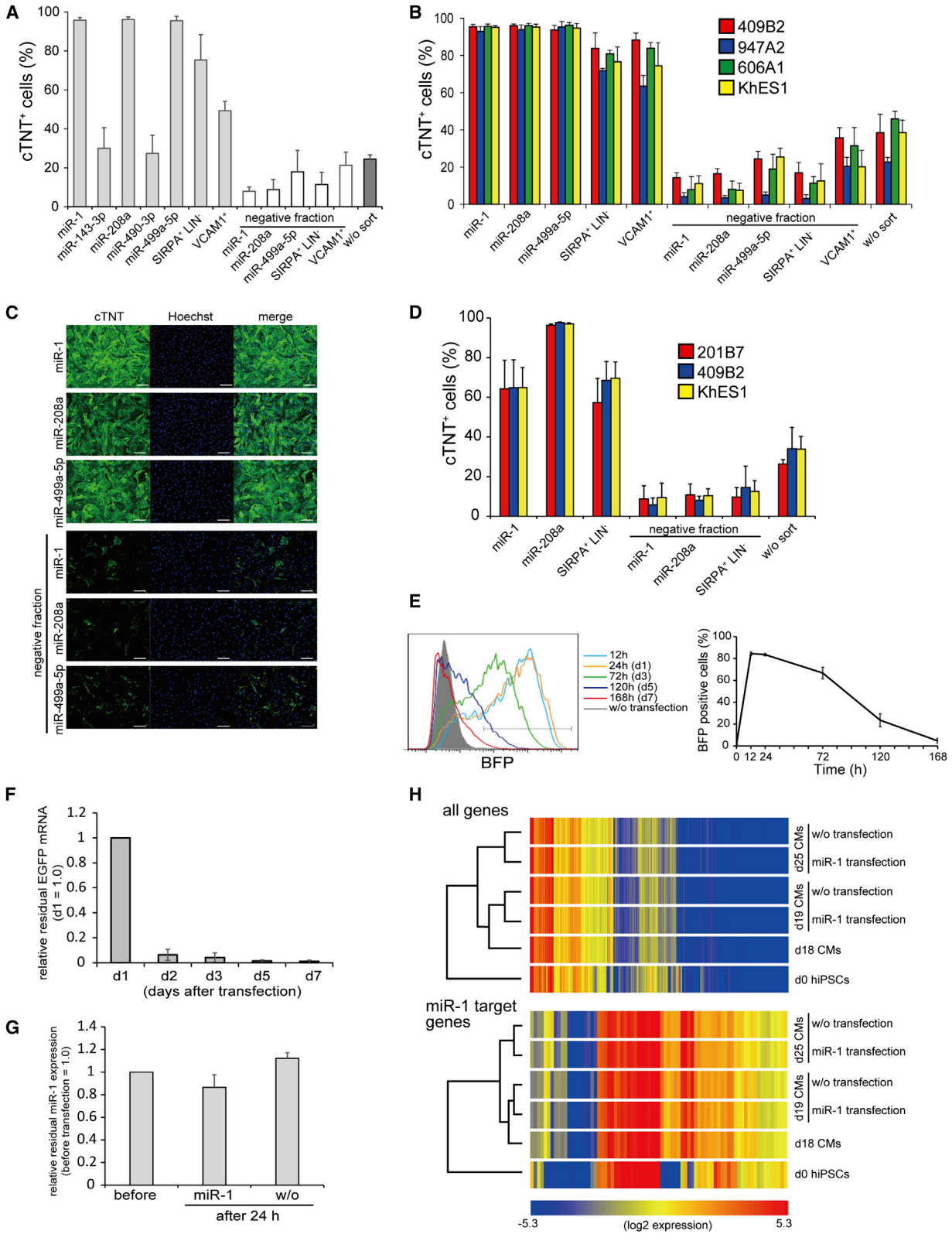

Figure 3. Purification of hPSC-Derived Cardiomyocytes Using miRNA Switches

(A and B) The average post-purification percentages of cTNT$^+$ cells from 201B7-derived cells (A, n = 3) and from cells derived from another four hPSC lines (B, n = 3–4) using several purification methods. The error bars represent the SD.

(legend continued on next page)

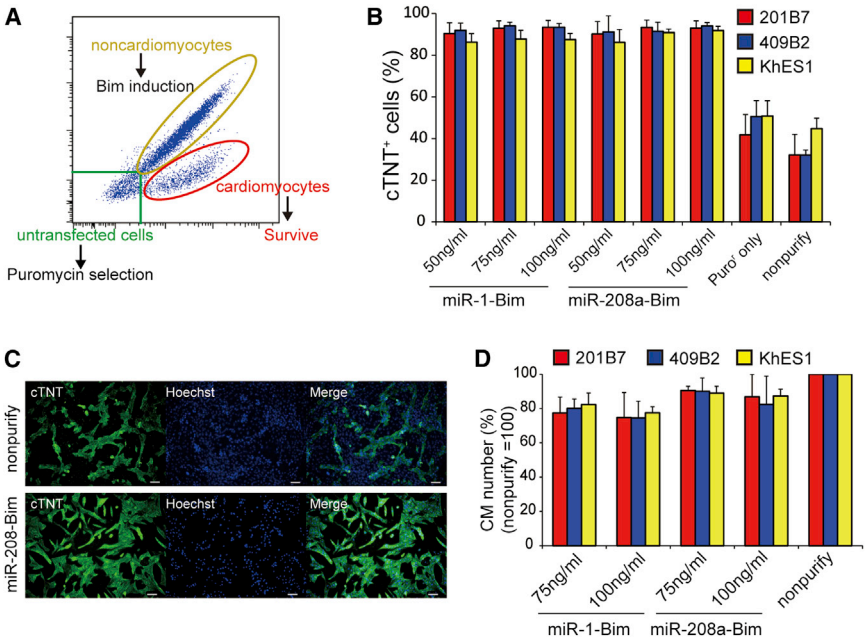

Figure 4. Non-Sorting System Using miRNA Switches Containing the Bim Sequence

(A) Scheme of cardiomyocyte purification using miR-Bim-switch and puromycin resistance mRNA selection.

(B) Average percentage of cTNT$^+$ cells after purification using miR-1-Bim-switch and miR-208a-Bim-switch in three hPSC lines. The error bars represent the SD (n = 3).

(C) Immunostaining for cTNT expression in non-purified and miR-208a-Bim-switch-purified cells. The nuclei were stained with Hoechst. Scale bars represent 100 μm.

(D) Recovery proportion of CMs using miR-Bim-switch. The recovery rate was calculated by dividing the cell number of each sample by the number of non-purified samples. The error bars represent the SD (n = 3).

See also Figure S4.

were robustly engrafted, survived in the heart, and expressed cTNT (Figure 5B). For functional restoration of the host heart in cardiac cell therapy, the transplanted cardiomyocytes should be well integrated with the host myocardium, and previous reports have highlighted the importance of gap junction formation for functional integration (Caspi et al., 2007; Gepstein et al., 2010). We thus evaluated the expression of Connexin 43 (Cx43), which is one of major components of gap junctions in ventricular myocardium. Immunostaining revealed Cx43 expression between the host heart and transplanted cells (Figures 5C–5F), suggesting the formation of gap junctions. Importantly, no tumor formation was observed in the transplanted hearts when the mice were sacrificed.

To further investigate the tumorigenicity of miRNA switch-purified cardiomyocytes, 2 × 10^4 hiPSCs (201B7), 2 × 10^5 201B7-derived non-purified cells, 2 × 10^5 miR-1-BFP-switch-sorted cardiomyocytes, or miR-208a-Bim-switch-purified cardiomyocytes were injected into the testes of immunodeficient (SCID) mice. Approximately 3 months later, we observed tumor formation in six of the six mice injected with hiPSCs, one of the eight mice injected with non-purified cells, and zero of eight mice injected with the miR-1-BFP-switch-sorted and miR-208a-Bim-purified cells (Figures 5G and H). Histological examination showed that the tumors generated by the hiPSCs (six of six) and non-purified cells (one of eight) contained tissues of the three embryonic germ layers (Figure S5A). In contrast, the tumor-free transplanted testes of the non-purified cell group (seven of eight), the miR-1-BFP-switch-sorted cell group (eight of eight), and miR-208a-Bim-purified cell group (eight of eight) were histologically similar to normal mouse testes (Figure S5B). Taken together, miRNA switch-purified cardiomyocytes were engrafted and survived in the hearts and did not form tumors, even when injected into the testes.

Purification of Endothelial Cells, Hepatocytes, and INSULIN-Producing Cells Derived from hPSCs Using miRNA Switches

An attractive feature of the miRNA switch is its availability in many types of cells. Therefore, we investigated whether cell-type-specific miRNA switches could purify endothelial cells, hepatocytes and INSULIN-producing cells derived from hPSCs. For endothelial cells, we selected specific miRNA candidates from pooled human umbilical vein endothelial cells (HUVECs) using miRNA microarray analysis and synthesized the top five miRNA switch candidates with BFP as the reporter again

(C) Immunohistochemical analysis of cTNT expression in miR-1-, miR-208a-, and miR-499a-5p-switch-sorted cells and in negative fraction cells. The nuclei were stained with Hoechst. Scale bars represent 100 μm.

(D) Average percentages of cTNT$^+$ cells after purification by several methods in three hPSC-derived cell lines at the early phase of differentiation. The error bars represent SD (n = 3).

(E) Flow cytometric analysis of BFP from 12 hr to day 7 after BFP mRNA transfection into day 18 EGFP$^+$ cardiomyocytes derived from MYH6-EIP4 hiPSCs. The error bars represent the SD (n = 3).

(F) Analysis of residual EGFP mRNA levels by qRT-PCR. The day after transfection, total RNA was extracted from part of the miR-1-switch-sorted cells as day 1 samples, and the other miR-1-switch-sorted cells were cultured for another 6 days. Total RNA was sampled on each day. The data are shown as the mean ± SD (n = 3).

(G) Analysis of endogenous miR-1 expression by qRT-PCR. The data are shown as the mean ± SD (n = 3).

(H) Hierarchical clustering of gene expression profiles of hiPSCs, day 18 cardiomyocytes (CMs), day 19 CMs with or without transfection on day 18, and day 25 CMs with or without transfection on day 18. EGFP$^+$ cardiomyocytes derived from MYH6-EIP4 hiPSCs were sorted on day 16 after the initiation of differentiation and cultured. miR-1-switch was transfected into the cells on day 18. miR-1 target genes were selected from miRTarBase (http://mirtarbase.mbc.nctu.edu.tw); n = 3.

See also Figures S2 and S3 and Table S1.

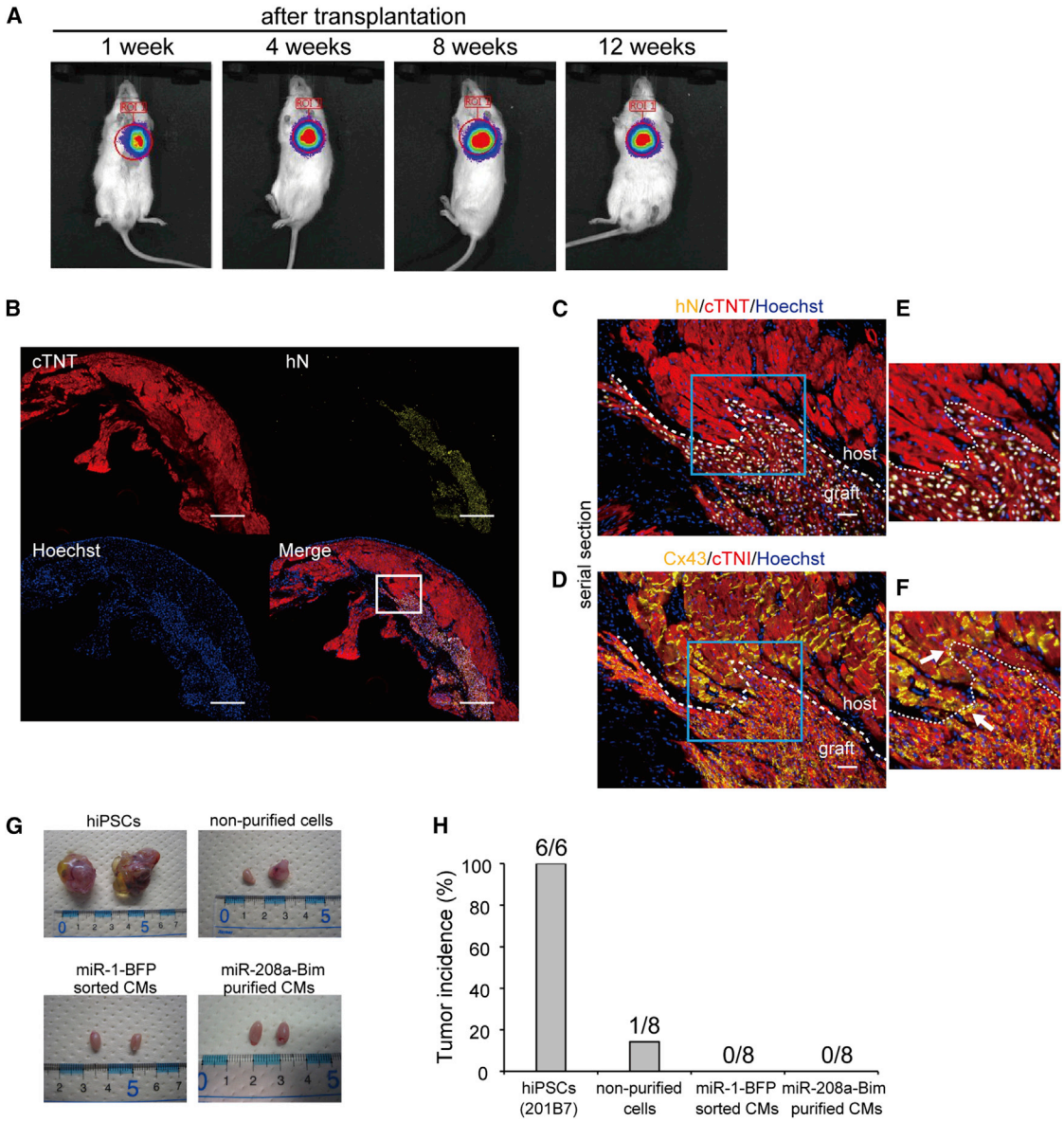

Figure 5. Transplantation of Purified Cardiomyocytes into Mouse Hearts and Testes

(A) Luciferase imaging by IVIS after the transplantation of miR-208a-Bim-switch-purified cardiomyocytes (n = 3).

(B) Representative immunostaining of heart sections for cTNT and human nuclei (hN) at approximately 3 months after transplantation. The nuclei were stained with Hoechst. Scale bars represent 500 μm.

(C) Magnification of (B). Scale bars represent 50 μm.

(D) Serial section image of (C). Immunostaining for Cx43 and cardiac Troponin I (cTNI). Scale bars represent 50 μm.

(E and F) Magnification of (C) and (D), respectively. White arrows point to the Cx43 expression between host and transplanted cardiomyocytes.

(G) Tumor formation capacities of 2×10^4 hiPSCs, 2×10^5 non-purified cells, 2×10^5 miR-1-BFP-sorted CMs, and miR-208a-Bim-purified CMs at approximately 3 months after transplantation into the testes.

(H) The graph represents the tumor incidences of each group (hiPSCs, n = 6; non-purified cells, n = 8; miR-1-BFP-sorted CMs, n = 8; miR-208a-Bim-purified CMs, n = 8).

See also Figure S5.

(Figures S6A and S6B). We transfected these miRNA switches individually with control EGFP mRNA into HUVECs and then confirmed that miR-126-3p- and miR-126-5p-switches reacted in the transfected HUVECs (Figure S6B). We next investigated whether miR-126-3p- and miR-126-5p-switches could isolate endothelial cells from hPSC-derived differentiated cells, which were induced using the same method for cardiomyocyte differentiation and which contained approximately 5%–10% $CD31^+$ cells: CD31 is a marker for endothelial cells. miR-126-3p- and miR-126-5p-switches allowed highly selective purification of $CD31^+$ cells from the heterogeneous cell populations of the four differentiated hPSC lines. In contrast, miR-208a-switch,

which enabled purification of cardiomyocytes, did not enrich CD31$^+$ cells, indicating high cell specificity for each of the miRNA switches (Figures 6A and 6B). In addition, a tube formation assay demonstrated that the cells sorted by miR-126-5p-switch had angiogenic potential (Figure 6C). For hepatocytes, we selected specific miRNA candidates from primary hepatocytes using miRNA microarray analysis and synthesized the top five miRNA switch candidates with BFP (Figure S6C). miR-122-5p-switch efficiently purified ALBUMIN$^+$ and HNF4A$^+$ hepatocytes derived from hiPSCs (Figures 6D and 6E). Immunostaining also confirmed that most of the cells sorted by miR-122-5p-switch were ALBUMIN$^+$ hepatocytes (Figure 6F). For INSULIN-producing cells, we selected several specific miRNA candidates from previous reports (Francis et al., 2014; Lahmy et al., 2014; Ozcan, 2014) because primary INSULIN-producing cells could not be obtained and there is no effective method to purify INSULIN-producing cells derived from hPSCs using specific surface markers. Interestingly, we found that miR-375-switch detected and separated part of the cells after the induction of INSULIN-producing cell differentiation using hiPSCs (Figure S6D). We sorted the detected cells and analyzed the cells by immunostaining; most of the sorted cells by miR-375-switch were INSULIN$^+$ cells (Figures 6G, 6H, and S6E). These results indicate that the miRNA switch approach is applicable to the purification of a variety of cell types, including cells in which specific surface markers have not been identified.

Simultaneous Purification of Cardiomyocytes and Endothelial Cells Using a Tandem miRNA Switch

Finally, we tested whether a single miRNA switch that responds to two miRNAs could simultaneously purify both cardiomyocytes and endothelial cells from a heterogeneous population derived from hPSCs. We synthesized four types of mRNA that included a tandem target miRNA sequence that combined miR-208a for cardiomyocytes with miR-126-3p and miR-126-5p for endothelial cells (Figure 7A). All four tandem miRNA switches purified cTNT$^+$ cardiomyocytes and CD31$^+$ endothelial cells effectively and simultaneously, although the BFP intensity in miR-126-5p+miR-208a-switch-transfected cells was weakly repressed compared with those cells transfected with the other three switches (Figures 7B and 7C).

DISCUSSION

In this study, we demonstrated that miRNA switches have great potential for the detection and purification of living target cells. Our designed miRNA switches allowed highly accurate and efficient isolation of functional cardiomyocytes derived from hPSCs. This system depends on only two distinct properties for purification: the miRNA switch is transfected into the cells, and specific miRNAs are used to identify the target cells. The simplicity of this method enables easy purification of desired cell types by employing appropriate miRNA switches. In addition, miR-Bim-switch, which selectively induces apoptosis in non-target cells, was used to purify cardiomyocytes without cell sorting (Figure 4B). Future clinical application of hPSC-derived cardiomyocytes requires large-scale purification that is not suitable for cell sorting. miR-Bim-switch not only provides high purity but also high yield, achieving an approximately 90% recovery rate for cardiomyocytes (Figure 4D). Thus, a system that controls apoptosis based on miRNA activity selectively kills non-target cells and autonomously recovers purified cardiomyocytes from a heterogeneous cell population.

During the screening of active miRNAs expressed in hPSC-derived cardiomyocytes, we found that miR-1-, miR-208a-, and miR-499a-5p-responsive mRNAs purified cardiomyocytes from five hPSC lines at more than 95% efficiency. The purity of the cardiomyocytes isolated by these miRNA switches was higher compared with those purified by previously reported methods using antibodies for cell surface markers (Dubois et al., 2011; Elliott et al., 2011; Uosaki et al., 2011). Furthermore, most of the unselected cardiomyocytes by these miRNA switches were non-transfected cells (Figure S2D). Thus, improvements in RNA transduction technology should lead to better efficiencies by the miRNA switch method outlined here. Interestingly, miR-208a-switch efficiently purified cardiomyocytes even during the early phase of differentiation, whereas miR-1-switch modestly enriched these cells, and miR-499a-5p-switch did not detect these cells, suggesting that the function of each miRNA switch is specific to the differentiation stage (Figure 3D). Such knowledge could be exploited further to isolate cardiomyocytes of varying stages of maturity, which may influence the efficacy of the subsequent transplantation.

There is a concern that the transfection of synthetic mRNA might provoke innate antiviral and toxic responses. We therefore used a modified RNA previously reported to minimize the immune response (Kormann et al., 2011; Warren et al., 2010; Zangi et al., 2013) and observed that most of the transfected mRNAs were degraded within 48 hr after transfection, such that endogenous miRNA was not depleted, and the miRNA switch did not significantly influence the global gene expression pattern or the miRNA-target genes (Figures 3E–3H). Furthermore, we confirmed that isolated cardiomyocytes were successfully engrafted and survived after their injection into the hearts of NOG mice (Figures 5A–5F). These data demonstrate the clinical potential of synthetic miRNA switches.

To isolate cardiomyocytes, we identified 14 candidate miRNAs, of which 8 miRNA switches did not react despite the different expression levels between cardiomyocytes and other cell types (Figure 2D). Similarly, we identified two miRNAs that could be used to purify endothelial cells among the five miRNAs that showed distinct expression patterns in the miRNA array. There are several possible explanations for the functional differences between miRNA switches. The miRNA array may have detected both active (high translational repression ability) and inactive (no translational repression ability) miRNAs expressed in the cells. In fact, miRNA sensor and decoy library-based studies have reported that more than 60% of detected miRNAs do not show discernible activity (Mullokandov et al., 2012). Another possibility is that the sequence of the miRNA (and its anti-sense) and the secondary structure of the miRNA switch may affect the affinity between the two RNAs. Understanding the responsible molecular mechanisms would expand the application of de novo miRNA switches for cell purification. Additionally, active miRNAs that distinguish target cells could be determined by a functional screening approach using the miRNA switch library.

In summary, we demonstrated that a miRNA switch system enables high purification of cardiomyocytes, endothelial cells,

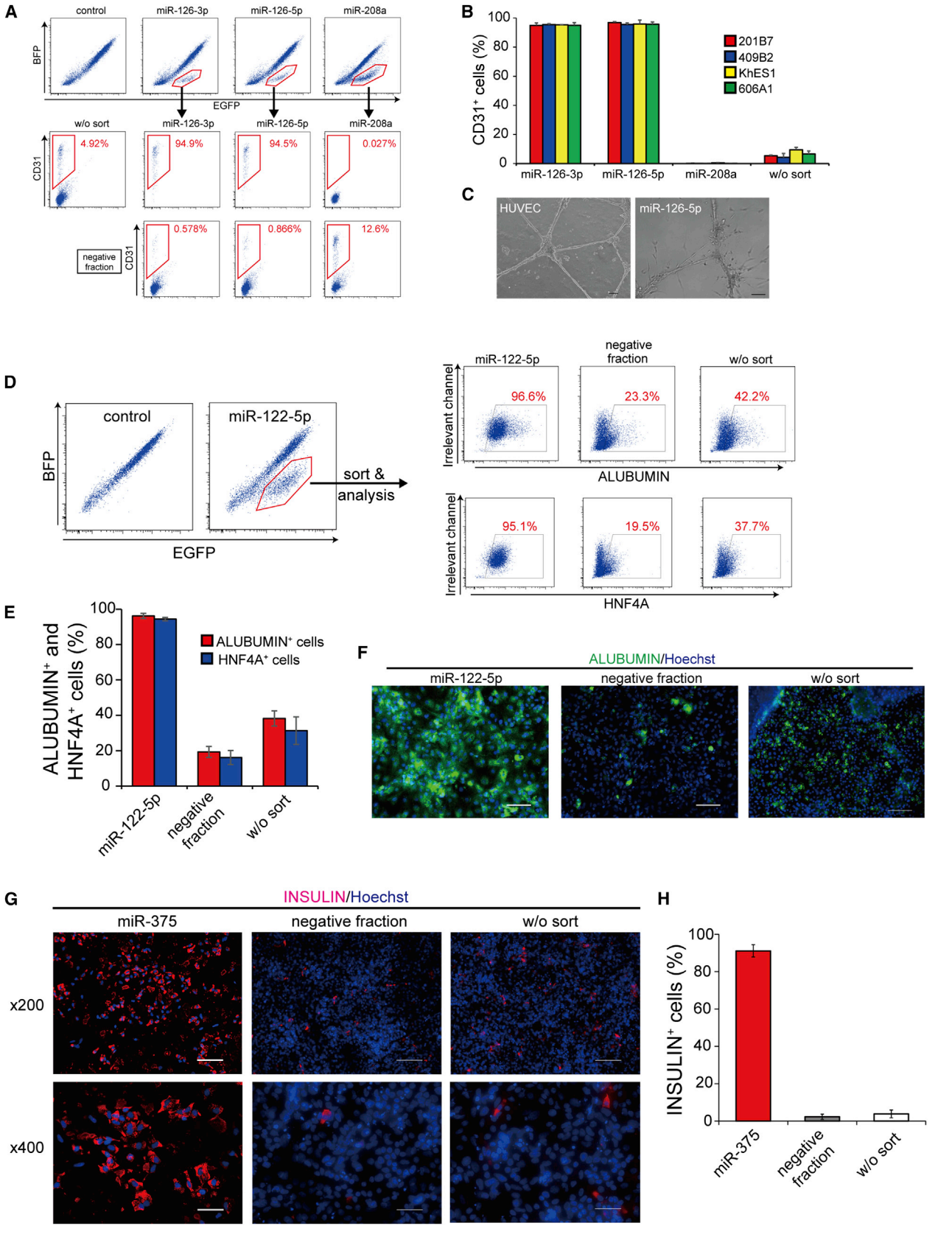

(legend on next page)

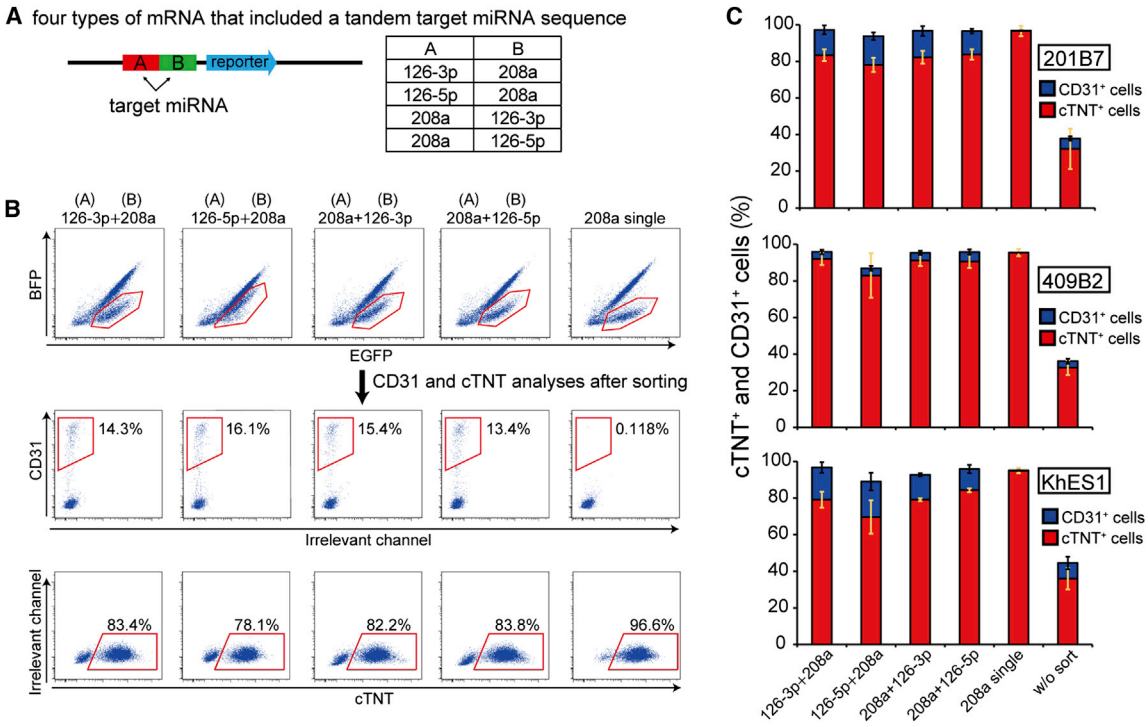

Figure 7. Simultaneous Purification of hPSC-Derived Cardiomyocytes and Endothelial Cells Using Tandem miRNA Switches

(A) Scheme of tandem miRNA switches.

(B) Representative flow cytometry plots of tandem miRNA switches expressed in 201B7-derived cells. The solid line represents the repressed BFP signal using each miRNA switch at day 20. BFP repression-sorted cells were analyzed by staining for CD31 and cTNT.

(C) The average percentages of $CD31^+$ and $cTNT^+$ cells in three hPSC-derived cells after purification by tandem miRNA switches. The error bars represent the SD (n = 3).

hepatocytes, and INSULIN-producing cells differentiated from hPSCs without affecting cellular properties. Its versatility and safety make this technology a promising tool for both basic and clinical stem cell research.

EXPERIMENTAL PROCEDURES

Plasmid Construction

The multiple cloning site of the pGEM T-easy vector (Promega) was modified to obtain a pAM empty vector via PCR-based site-directed mutagenesis using the primer set FwdMCS and RevMCS. Next, the protein-coding region of EGFP (Clontech) or tagBFP (Evrogen) was amplified via PCR using the primer sets CFwdEGFP and CRevEGFP or CFwdtagBFP and CRevtagBFP. The PCR products were digested with NcoI and BglII and inserted into the NcoI and BglII sites of pAM to obtain pAM-EGFP and pAM-tagBFP. To generate 5′ UTRs containing the miR-21-5p or miR-17-5p target site, pairs of oligo-DNAs, 5Tmi21_Afwd and 5Tmi21_Arev or 5Tmi17_5_Afwd and 5Tmi17_5_Arev, were annealed and inserted into the BamHI and AgeI sites of 18nt-2xFr15-ECFP (Endo et al., 2013). Then, the 5′ UTR was amplified using the primer set T7FwdA and Rev5′ UTR. The primer sequences and the PCR reaction conditions are provided in Tables S2 and S3, respectively.

Preparation of Template DNA for IVT

5′ and 3′ UTRs without miRNA target sequences (control UTRs) and the protein-coding regions of reporter mRNAs were prepared by PCR with proper

Figure 6. Purification of Endothelial Cells, Hepatocytes, and INSULIN-Producing Cells Derived from hPSCs Using miRNA Switches

(A) Representative flow cytometry plots of miR-126-3p-, miR-126-5p-, and miR-208a-switches in 201B7-derived cells at day 20. The solid line represents the repressed BFP signal for each miRNA switch. After sorting the cells in the repressed BFP signal and negative fraction, the cells were analyzed by CD31 staining.

(B) The average percentages of $CD31^+$ cells after purification by miR-126-3p-, miR-126-5p-, and miR-208a-switches in four hPSC-derived cells. The error bars represent the SD (n = 3).

(C) Tube formation assay of HUVECs and miR-126-5p-switch-purified endothelial cells derived from hPSCs. Scale bars represent 100 μm.

(D) Left: representative flow cytometry plots of miR-122-5p-switch-transfected cells derived from a hiPSC clone (201B6) at day 17. Right: after sorting the cells in the repressed BFP signal and negative fraction, the cells were analyzed by staining for ALBUMIN and HNF4A.

(E) The average percentages of $ALBUMIN^+$ and $HNF4A^+$ cells in 201B6-derived cells after purification by miR-122-5p-switch. The error bars represent the SD (n = 3).

(F) Immunohistochemical analysis of ALBUMIN expression in miR-122-5p-switch-sorted cells, negative fraction cells and non-sorted cells. The nuclei were stained with Hoechst. Scale bars represent 100 μm.

(G) Immunohistochemical analysis of INSULIN expression in miR-375-switch-sorted cells derived from a hiPSC clone (585A1) at day 18, negative fraction cells, and non-sorted cells. The nuclei were stained with Hoechst. Scale bars represent 100 μm (top) and 50 μm (bottom).

(H) The average percentage of $INSULIN^+$ cells after purification by miR-375-switch. The error bars represent the SD (n = 3).

See also Figure S6.

primer sets from plasmids and synthesized oligo-DNAs, respectively. The PCR fragments of the 5′ UTR (10 pmol), a coding region (50 ng), and the 3′ UTR (10 pmol) were fused to generate DNA templates for IVT via a further PCR reaction with the primer set T7FwdG3C (or T7FwdA) and Rev120A. Oligo-DNAs and the T7FwdB primer were also used in the fusion PCR instead of the PCR products of the UTRs or T7Fwd5UTR primer, respectively. The primer sequences and the PCR reaction conditions are provided in Tables S2 and S3, respectively.

The PCR products were purified using a MinElute PCR purification kit (QIAGEN) according to the manufacturer's instructions. Before purification, the PCR products amplified from plasmids were subjected to digestion with the *Dpn* I restriction enzyme (Toyobo) for 30 min at 37°C.

mRNA Synthesis and Purification

miRNA-responsive mRNAs were generated using a MegaScript T7 kit (Ambion) and a modified protocol (Warren et al., 2010). In the reaction, pseudouridine-5′-triphosphate and 5-methylcytidine-5′-triphosphate (TriLink BioTechnologies) were used instead of uridine triphosphate and cytosine triphosphate, respectively. Guanosine-5′-triphosphate was 5-fold diluted with Anti-Reverse Cap Analog (New England Biolabs) before the IVT reaction. Reaction mixtures were incubated at 37°C for 4 hr, mixed with TURBO DNase (Ambion), and further incubated at 37°C for 30 min. The resulting mRNAs were purified using a FavorPrep Blood/Cultured Cells total RNA extraction column (Favorgen Biotech), incubated with Antarctic Phosphatase (New England Biolabs) at 37°C for 30 min, and then purified again using an RNeasy MiniElute Cleanup Kit (QIAGEN).

miRNA and mRNA Microarray Analysis

miRNA and mRNA expression profiling was performed using the Agilent Technologies Human miRNA Microarray Release 19.0 and the SurePrint G3 Human GE Microarray according to the manufacturers' protocols, respectively. The data were analyzed using GeneSpring GX 12.6 software (Agilent Technologies).

Reverse Transcription and qPCR

For the detection of mRNA transcripts, purified RNA was reverse transcribed using a ReverTra Ace-α-kit (Toyobo) with the oligo(dT)20 primer. For miRNA, purified total RNA was reverse transcribed using miR-1 and RNU6B Taqman probes (Applied Biosystems). Quantitative PCR (qPCR) was performed with the Taqman probes, and the samples were analyzed using a StepOne Plus Real-Time PCR System (Applied Biosystems). The Taqman probes are shown in Table S4.

Tube Formation Assay

HUVEC and miR-126-5p-switch-sorted cells were seeded in a Matrigel-coated 24-well plate at 2 × 10^5 cells/well in EGM-2 BulletKit medium. The next day, images of the samples were acquired using a Biorevo BZ-9000 microscope.

Statistical Analysis

The data are presented as the means and SDs of the experiments. Student's t test was used for the statistical analysis.

ACCESSION NUMBERS

The microarray data reported in this paper have been deposited in GEO under accession number GEO: GSE60633.

SUPPLEMENTAL INFORMATION

Supplemental Information includes Supplemental Experimental Procedures, six figures, and four tables and can be found with this article online at http://dx.doi.org/10.1016/j.stem.2015.04.005.

AUTHOR CONTRIBUTIONS

K.M., K.E., S.Y., Y.Y., and H.S. conceived and designed the project. K.M., K.E., S.T., S.F., I.T., S.K., T.T., M.K., T.T., M.U., C.O., M.N., A.O., M.N., I.M., K.A., K.H., and K.O. performed the experimental work. K.M and K.E. analyzed the data. K.M, K.E., H.S., and Y.Y. wrote the manuscript. All authors discussed the results.

ACKNOWLEDGMENTS

The authors are grateful to Gordon Keller and Mark Gagliardi (University Health Network) for providing valuable advice and support for the cardiomyocyte differentiation method. We thank Nanaka Nishimura and Shunnichi Kashida (Kyoto University) for preparing some of the materials and for critical comments on the project, respectively. We also thank Yasuhiro Yamada, Takuya Yamamoto, Callum Parr, and Peter Karagiannis (Kyoto University) for critical reading of the manuscript. We are grateful to Rie Kato, Sayaka Takeshima, Eri Nishikawa, Ryoko Fujiwara, Kyoko Nakahara, Yukiko Nakagawa, and Yoko Miyake for their administrative support. This research was funded by the Japan Society for the Promotion of Science (JSPS) through the "Funding Program for World-Leading Innovative R&D on Science and Technology (FIRST program)" initiated by the Council for Science and Technology Policy (CSTP) (to S.Y.), the Balzan Prize assigned to S.Y. and H.S., Health and Labour Sciences Research Grants from the Ministry of Health Labour and Welfare (to Y.Y.), grants from the Research Center Network for Realization of Regenerative Medicine (to H.S., Y.Y., and S.Y.), and the iPS Cell Research Fund. A part of this study was supported by JSPS KAKENHI grant numbers 24790277 (to Y.Y.), 25870355 (to K.E.), and 23681042 and 24104002 (to H.S.). S.Y. is a scientific advisor of iPS Academia Japan without salary and K.O. is a member without salary of the scientific advisory boards of iPS Portal, Japan. Kyoto University has filed a patent application broadly relevant to this work. K.E., K.M., S.T., Y.Y., and H.S. are the investigators of record listed on the patent application.

Received: September 30, 2014
Revised: February 26, 2015
Accepted: April 13, 2015
Published: May 21, 2015

REFERENCES

Anderson, D., Self, T., Mellor, I.R., Goh, G., Hill, S.J., and Denning, C. (2007). Transgenic enrichment of cardiomyocytes from human embryonic stem cells. Mol. Ther. *15*, 2027–2036.

Ban, K., Wile, B., Kim, S., Park, H.J., Byun, J., Cho, K.W., Saafir, T., Song, M.K., Yu, S.P., Wagner, M., et al. (2013). Purification of cardiomyocytes from differentiating pluripotent stem cells using molecular beacons that target cardiomyocyte-specific mRNA. Circulation *128*, 1897–1909.

Bizy, A., Guerrero-Serna, G., Hu, B., Ponce-Balbuena, D., Willis, B.C., Zarzoso, M., Ramirez, R.J., Sener, M.F., Mundada, L.V., Klos, M., et al. (2013). Myosin light chain 2-based selection of human iPSC-derived early ventricular cardiac myocytes. Stem Cell Res. (Amst.) *11*, 1335–1347.

Caspi, O., Huber, I., Kehat, I., Habib, M., Arbel, G., Gepstein, A., Yankelson, L., Aronson, D., Beyar, R., and Gepstein, L. (2007). Transplantation of human embryonic stem cell-derived cardiomyocytes improves myocardial performance in infarcted rat hearts. J. Am. Coll. Cardiol. *50*, 1884–1893.

Dubois, N.C., Craft, A.M., Sharma, P., Elliott, D.A., Stanley, E.G., Elefanty, A.G., Gramolini, A., and Keller, G. (2011). SIRPA is a specific cell-surface marker for isolating cardiomyocytes derived from human pluripotent stem cells. Nat. Biotechnol. *29*, 1011–1018.

Elliott, D.A., Braam, S.R., Koutsis, K., Ng, E.S., Jenny, R., Lagerqvist, E.L., Biben, C., Hatzistavrou, T., Hirst, C.E., Yu, Q.C., et al. (2011). NKX2-5(eGFP/w) hESCs for isolation of human cardiac progenitors and cardiomyocytes. Nat. Methods *8*, 1037–1040.

Endo, K., Stapleton, J.A., Hayashi, K., Saito, H., and Inoue, T. (2013). Quantitative and simultaneous translational control of distinct mammalian mRNAs. Nucleic Acids Res. *41*, e135.

Francis, N., Moore, M., Rutter, G.A., and Burns, C. (2014). The role of microRNAs in the pancreatic differentiation of pluripotent stem cells. Microrna *3*, 54–63.

Garbern, J.C., and Lee, R.T. (2013). Cardiac stem cell therapy and the promise of heart regeneration. Cell Stem Cell *12*, 689–698.

Gepstein, L., Ding, C., Rahmutula, D., Wilson, E.E., Yankelson, L., Caspi, O., Gepstein, A., Huber, I., and Olgin, J.E. (2010). In vivo assessment of the electrophysiological integration and arrhythmogenic risk of myocardial cell transplantation strategies. Stem Cells *28*, 2151–2161.

Hattori, F., Chen, H., Yamashita, H., Tohyama, S., Satoh, Y.S., Yuasa, S., Li, W., Yamakawa, H., Tanaka, T., Onitsuka, T., et al. (2010). Nongenetic method for purifying stem cell-derived cardiomyocytes. Nat. Methods *7*, 61–66.

Kawamura, M., Miyagawa, S., Fukushima, S., Saito, A., Miki, K., Ito, E., Sougawa, N., Kawamura, T., Daimon, T., Shimizu, T., et al. (2013). Enhanced survival of transplanted human induced pluripotent stem cell-derived cardiomyocytes by the combination of cell sheets with the pedicled omental flap technique in a porcine heart. Circulation *128* (11, Suppl 1), S87–S94.

Khalil, A.S., and Collins, J.J. (2010). Synthetic biology: applications come of age. Nat. Rev. Genet. *11*, 367–379.

Kormann, M.S., Hasenpusch, G., Aneja, M.K., Nica, G., Flemmer, A.W., Herber-Jonat, S., Huppmann, M., Mays, L.E., Illenyi, M., Schams, A., et al. (2011). Expression of therapeutic proteins after delivery of chemically modified mRNA in mice. Nat. Biotechnol. *29*, 154–157.

Kozomara, A., and Griffiths-Jones, S. (2011). miRBase: integrating microRNA annotation and deep-sequencing data. Nucleic Acids Res. *39*, D152–D157.

Laflamme, M.A., Chen, K.Y., Naumova, A.V., Muskheli, V., Fugate, J.A., Dupras, S.K., Reinecke, H., Xu, C., Hassanipour, M., Police, S., et al. (2007). Cardiomyocytes derived from human embryonic stem cells in pro-survival factors enhance function of infarcted rat hearts. Nat. Biotechnol. *25*, 1015–1024.

Lahmy, R., Soleimani, M., Sanati, M.H., Behmanesh, M., Kouhkan, F., and Mobarra, N. (2014). MiRNA-375 promotes beta pancreatic differentiation in human induced pluripotent stem (hiPS) cells. Mol. Biol. Rep. *41*, 2055–2066.

Leisner, M., Bleris, L., Lohmueller, J., Xie, Z., and Benenson, Y. (2010). Rationally designed logic integration of regulatory signals in mammalian cells. Nat. Nanotechnol. *5*, 666–670.

Li, Z., Hu, S., Ghosh, Z., Han, Z., and Wu, J.C. (2011). Functional characterization and expression profiling of human induced pluripotent stem cell- and embryonic stem cell-derived endothelial cells. Stem Cells Dev. *20*, 1701–1710.

Mullokandov, G., Baccarini, A., Ruzo, A., Jayaprakash, A.D., Tung, N., Israelow, B., Evans, M.J., Sachidanandam, R., and Brown, B.D. (2012). High-throughput assessment of microRNA activity and function using microRNA sensor and decoy libraries. Nat. Methods *9*, 840–846.

Osborn, L., Hession, C., Tizard, R., Vassallo, C., Luhowskyj, S., Chi-Rosso, G., and Lobb, R. (1989). Direct expression cloning of vascular cell adhesion molecule 1, a cytokine-induced endothelial protein that binds to lymphocytes. Cell *59*, 1203–1211.

Ozcan, S. (2014). Minireview: microRNA function in pancreatic β cells. Mol. Endocrinol. *28*, 1922–1933.

Rinaudo, K., Bleris, L., Maddamsetti, R., Subramanian, S., Weiss, R., and Benenson, Y. (2007). A universal RNAi-based logic evaluator that operates in mammalian cells. Nat. Biotechnol. *25*, 795–801.

Takahashi, K., Tanabe, K., Ohnuki, M., Narita, M., Ichisaka, T., Tomoda, K., and Yamanaka, S. (2007). Induction of pluripotent stem cells from adult human fibroblasts by defined factors. Cell *131*, 861–872.

Tohyama, S., Hattori, F., Sano, M., Hishiki, T., Nagahata, Y., Matsuura, T., Hashimoto, H., Suzuki, T., Yamashita, H., Satoh, Y., et al. (2013). Distinct metabolic flow enables large-scale purification of mouse and human pluripotent stem cell-derived cardiomyocytes. Cell Stem Cell *12*, 127–137.

Uosaki, H., Fukushima, H., Takeuchi, A., Matsuoka, S., Nakatsuji, N., Yamanaka, S., and Yamashita, J.K. (2011). Efficient and scalable purification of cardiomyocytes from human embryonic and induced pluripotent stem cells by VCAM1 surface expression. PLoS ONE *6*, e23657.

Warren, L., Manos, P.D., Ahfeldt, T., Loh, Y.H., Li, H., Lau, F., Ebina, W., Mandal, P.K., Smith, Z.D., Meissner, A., et al. (2010). Highly efficient reprogramming to pluripotency and directed differentiation of human cells with synthetic modified mRNA. Cell Stem Cell *7*, 618–630.

White, M.P., Rufaihah, A.J., Liu, L., Ghebremariam, Y.T., Ivey, K.N., Cooke, J.P., and Srivastava, D. (2013). Limited gene expression variation in human embryonic stem cell and induced pluripotent stem cell-derived endothelial cells. Stem Cells *31*, 92–103.

Xie, Z., Wroblewska, L., Prochazka, L., Weiss, R., and Benenson, Y. (2011). Multi-input RNAi-based logic circuit for identification of specific cancer cells. Science *333*, 1307–1311.

Xu, C., Police, S., Rao, N., and Carpenter, M.K. (2002). Characterization and enrichment of cardiomyocytes derived from human embryonic stem cells. Circ. Res. *91*, 501–508.

Yang, L., Soonpaa, M.H., Adler, E.D., Roepke, T.K., Kattman, S.J., Kennedy, M., Henckaerts, E., Bonham, K., Abbott, G.W., Linden, R.M., et al. (2008). Human cardiovascular progenitor cells develop from a KDR+ embryonic-stem-cell-derived population. Nature *453*, 524–528.

Ye, H., Aubel, D., and Fussenegger, M. (2013). Synthetic mammalian gene circuits for biomedical applications. Curr. Opin. Chem. Biol. *17*, 910–917.

Yu, J., Vodyanik, M.A., Smuga-Otto, K., Antosiewicz-Bourget, J., Frane, J.L., Tian, S., Nie, J., Jonsdottir, G.A., Ruotti, V., Stewart, R., et al. (2007). Induced pluripotent stem cell lines derived from human somatic cells. Science *318*, 1917–1920.

Zangi, L., Lui, K.O., von Gise, A., Ma, Q., Ebina, W., Ptaszek, L.M., Später, D., Xu, H., Tabebordbar, M., Gorbatov, R., et al. (2013). Modified mRNA directs the fate of heart progenitor cells and induces vascular regeneration after myocardial infarction. Nat. Biotechnol. *31*, 898–907.

Zhang, D.Y., and Seelig, G. (2011). Dynamic DNA nanotechnology using strand-displacement reactions. Nat. Chem. *3*, 103–113.

Cell Stem Cell

Supplemental Information

Efficient Detection and Purification of Cell Populations Using Synthetic MicroRNA Switches

Kenji Miki, Kei Endo, Seiya Takahashi, Shunsuke Funakoshi, Ikue Takei, Shota Katayama, Taro Toyoda, Maki Kotaka, Tadashi Takaki, Masayuki Umeda, Chikako Okubo, Misato Nishikawa, Akiko Oishi, Megumi Narita, Ito Miyashita, Kanako Asano, Karin Hayashi, Kenji Osafune, Shinya Yamanaka, Hirohide Saito, and Yoshinori Yoshida

Supplementary Figures

Figure S1, related to Figure 2

Sorting and cTNT analysis of EGFP+ cells derived from the MYH6-EIP4 line at day 8 and day 20.

Figure S2, related to Figure 3

Representative flow cytometry plots and gating strategy for sorting hPSC-derived cells at day 20.

Figure S3, related to Figure 3

Characterization of miRNA switch-sorted cells.

Figure S4, related to Figure 4

Optimal concentration of puromycin and puromycin resistance mRNA for the non-sorting selection system.

Figure S5, related to Figure 5

Hematoxylin and eosin (HE) staining of teratomas and testes.

Figure S6, related to Figure 6

miRNA microarray analysis and miRNA switch transfection.

Supplementary Tables

Table S1, related to Figure 3

$cTNT^+$ percentages in 4 hPSC lines after sorting by miRNA switches or antibodies.

Table S2, related to Experimental Procedures

Primer list.

Table S3, related to Experimental Procedures

The PCR reaction conditions.

Table S4, related to Experimental Procedures

List of Taqman probes.

Supplementary Methods

Supplementary References

Supplementary Figure

Figure S1, related to Figure 2

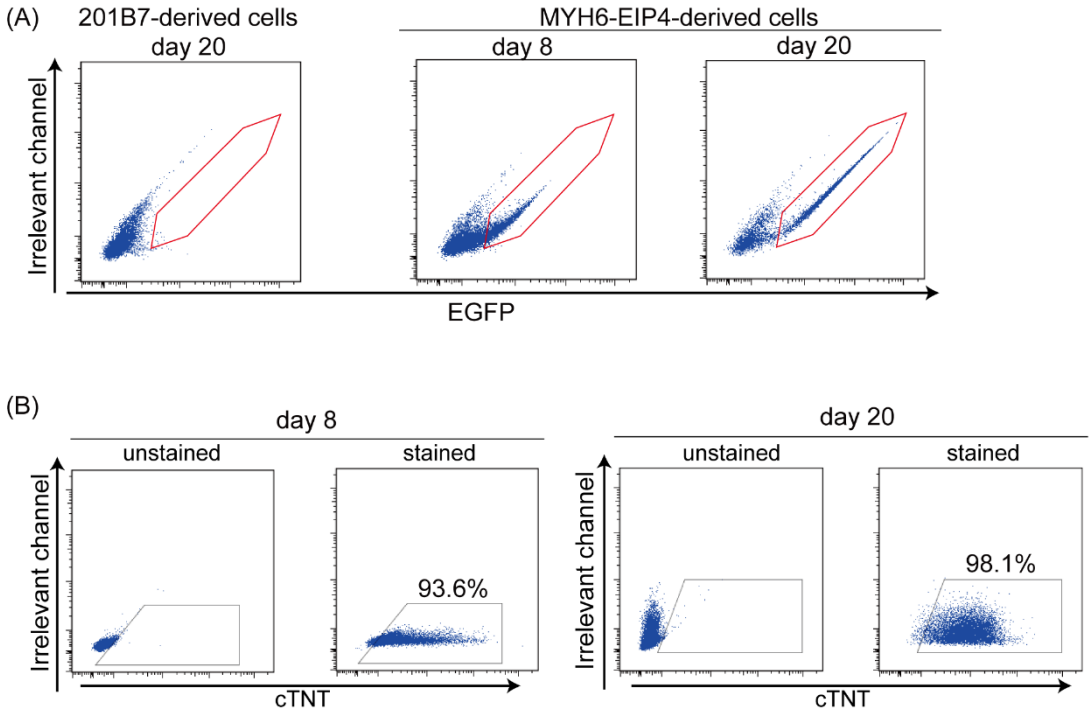

Figure S1, related to Figure 2

Sorting and cTNT analysis of EGFP+ cells derived from the MYH6-EIP4 line at day 8 and day 20. (**a**) EGFP$^+$ cells at day 8 and day 20. EGFP was not expressed in 201B7-derived cells at day 20. (**b**) cTNT analysis of sorted EGFP$^+$ cells from MYH6-EIP4 iPSCs at day 8 and day 20.

Figure S2, related to Figure 3

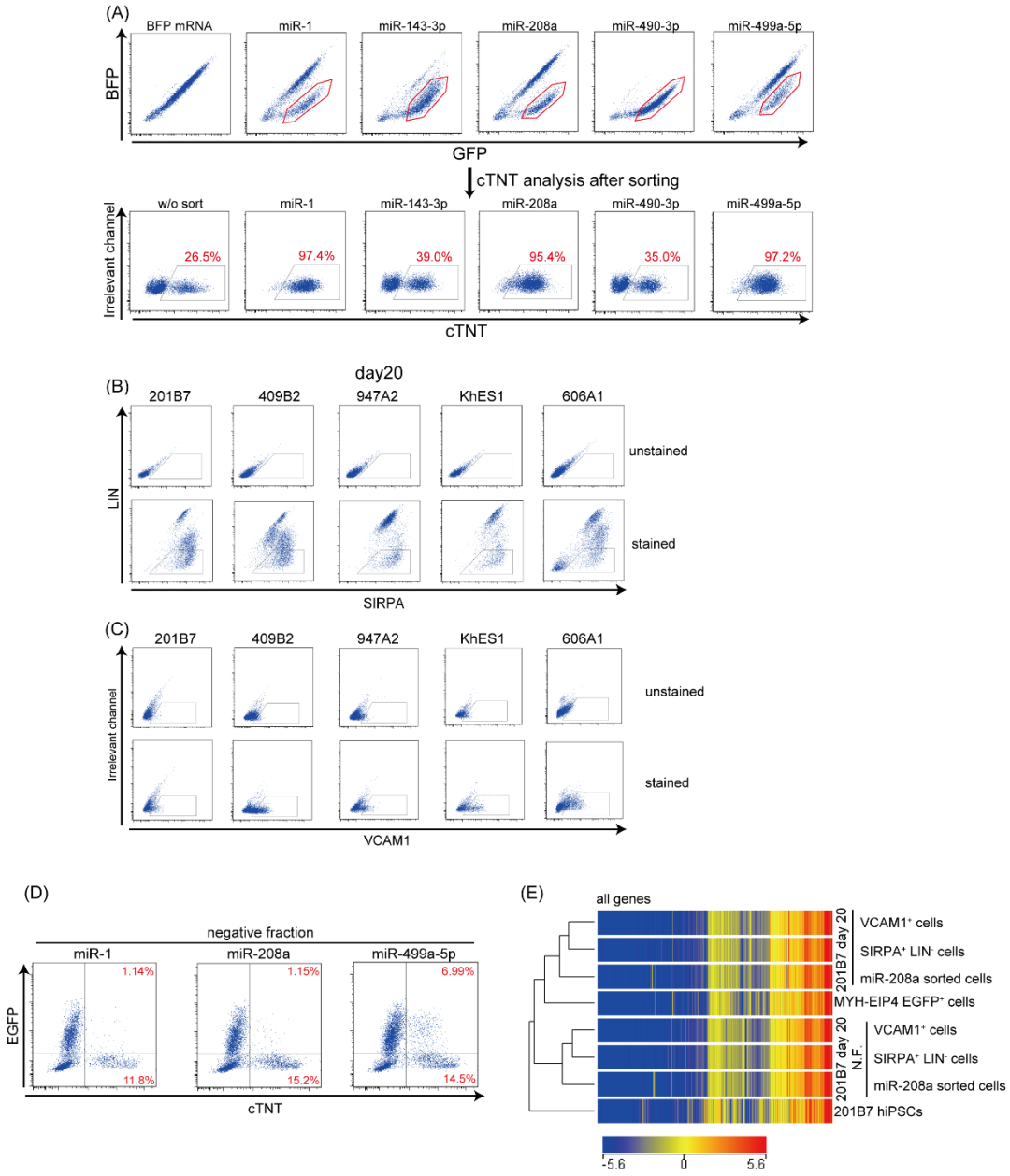

Figure S2, related to Figure 3

Representative flow cytometry plots and gating strategy for sorting of hPSC-derived cells at day 20. (**A**) Representative plots showing gating of miRNA switches in 201B7-derived cells and cTNT analysis of sorted cells. (**B, C**) Representative plots showing the gating of SIRPA$^+$ LIN$^-$ (**B**) and VCAM1$^+$ (**C**) in 5 hPSC lines. (**D**) Representative cTNT analysis of cells in the negative fraction of 201B7-derived cells transfected with miR-BFP-switch and EGFP mRNA. (**E**) Hierarchical clustering of gene expression profiles of day 20 cells sorted by miR-208a-switch and by SIRPA$^+$ LIN$^-$ and VCAM1$^+$ and of negative fraction (N.F.) cells and hiPSCs (201B7).

Figure S3, related to Figure 3

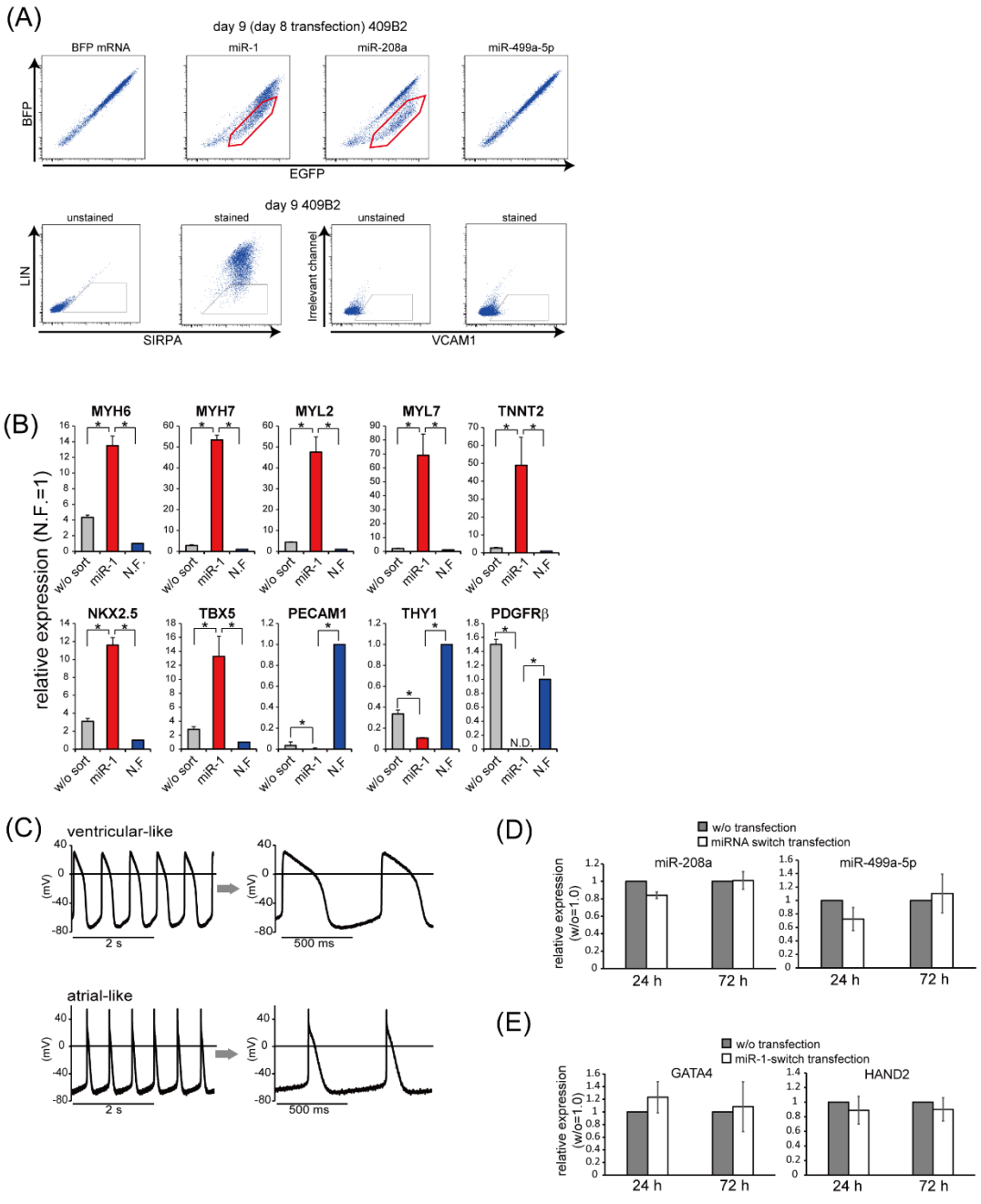

Figure S3, related to Figure 3

Characterization of miRNA switch-sorted cells. (**A**) Representative flow cytometry plots showing the gating of miRNA switches, SIRPA^{+}LIN^{-} area and VCAM1^{+} area in 409B2-derived cells at day 9. (**B**) qRT-PCR analysis of unsorted cells, miR-1-switch-sorted cells and N.F. cells. Cardiac-related gene expression (MYH6, MYH7, MYL2, MYL7, TNNT2, NKX2.5 and TBX5) was significantly higher in miR-1-sorted cells than in other cells. Non-cardiac gene expression (PECAM1, THY1 and PEGFRβ) was significantly lower in miR-1-sorted cells than in other cells.

The data are presented as the mean±SD. *, p≤0.01; *n*=3. (**C**) Representative action potentials recorded from miR-1-switch-sorted cardiomyocytes derived from the 201B7 cell line. (**D**) qRT-PCR analysis of endogenous miR-208a and miR-499a-5p expression 24 and 72 h after transfection with and without miRNA switch. The data are shown as the mean±SD (*n*=3). (E) qRT-PCR analysis of the expression of GATA4 and HAND2 at 24 and 72 h after transfection with and without miR-1-switch. The data are shown as the mean±SD (*n*=3).

Figure S4, related to Figure 4

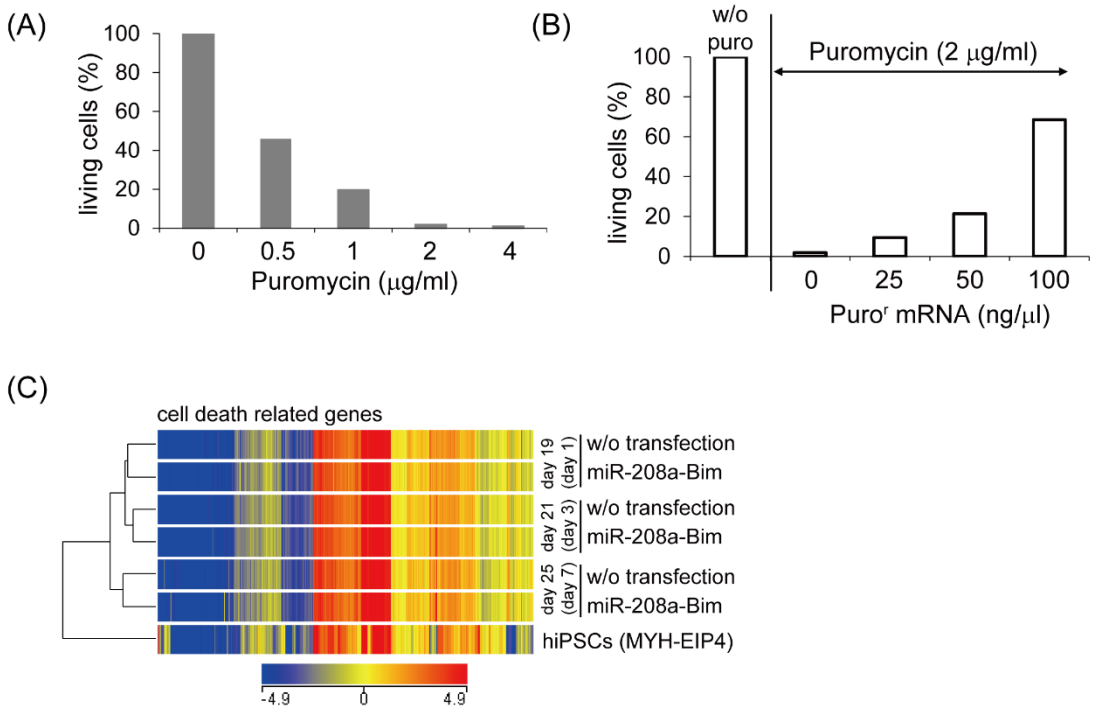

Figure S4, related to Figure 4

Optimal concentration of puromycin and puromycin resistance mRNA for the non-sorting selection system. (**A**) The effect of different puromycin concentrations on 409B2-derived cells at day 18. (**B**) The protective effect of different concentrations of puromycin resistance mRNA on puromycin-treated cells. (**C**) Hierarchical clustering of gene expression profiles of hiPSCs (MYH-EIP4), day 19 CMs with or without transfection on day 18, day 21 CMs with or without transfection on day 18 and day 25 CMs with or without transfection on day 18. $EGFP^+$ cardiomyocytes derived from MYH6-EIP4 hiPSCs were sorted on day 16 after differentiation initiation and cultured. miR-208a-Bim-switch was transfected into the cells on day 18. Cell death related genes were selected from the Gene Ontology Consortium (GO: 0008219 cell death, URL; http://geneontology.org/); *n*=3.

Figure S5, related to Figure 5

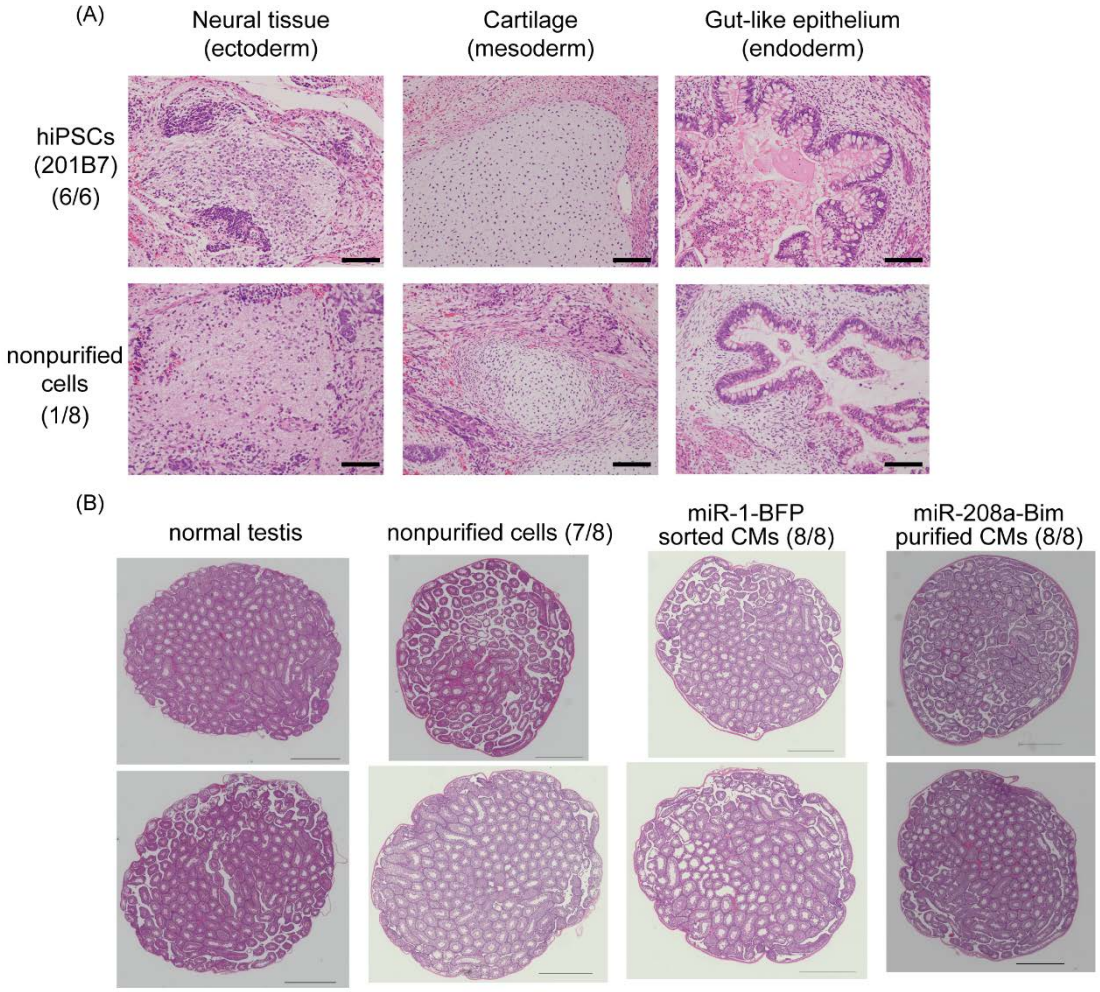

Figure S5, related to Figure 5
Hematoxylin and eosin (H&E) staining of teratomas and testes. (**A**) Representative images of hiPSC- and non-purified cell-derived teratomas containing the tissues of three embryonic germ layers. Scale bars, 100 μm. (**B**) Representative images of normal and each transplanted testes. Scale bars, 1 mm. *n*=8 per group.

Figure S6, related to Figure 6

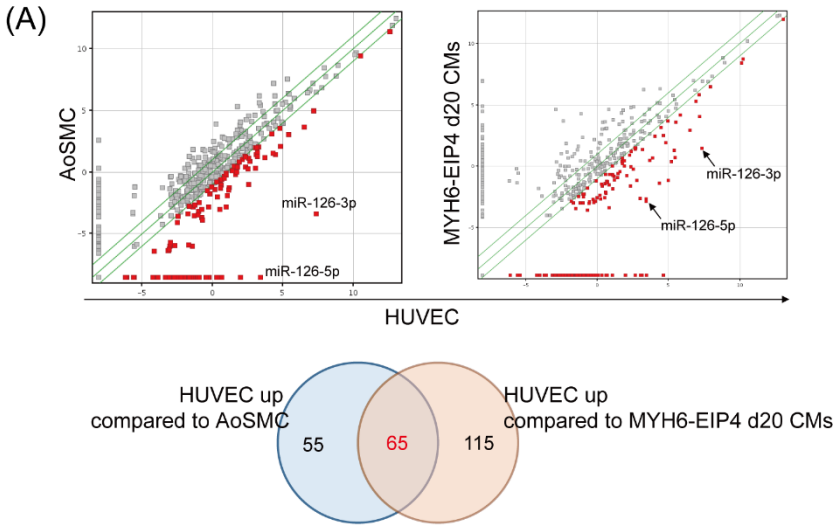

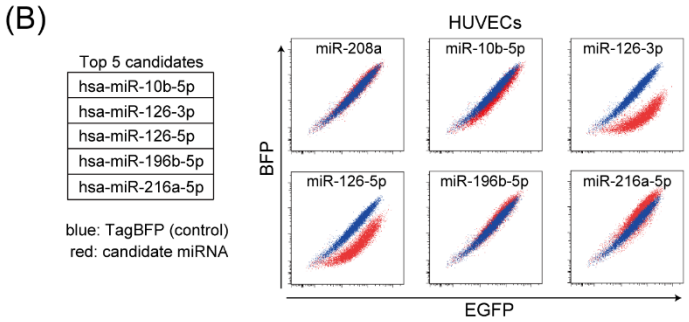

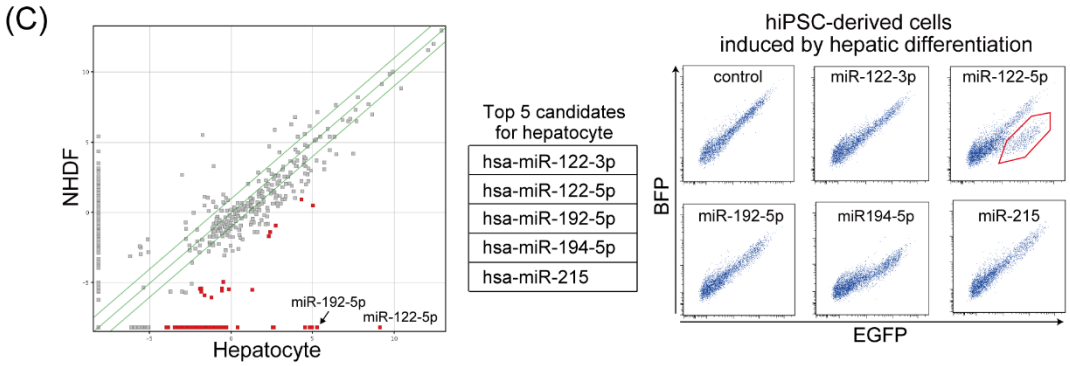

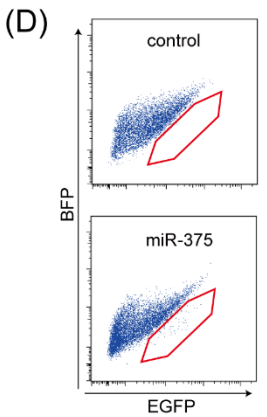

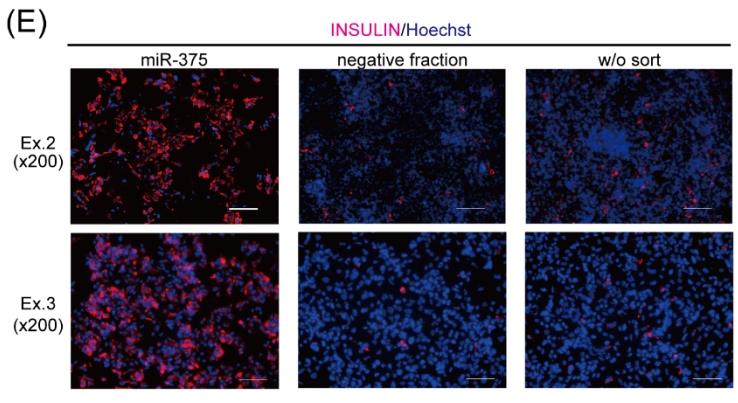

Figure S6, related to Figure 6

miRNA microarray analysis and miRNA switch transfection. (**A**) Scatter plots comparing gene expression between HUVECs and AoSMCs (left) and between HUVECs and MYH6-EIP4 day 20 CMs (right) by microarray analysis. In total, 65 miRNAs were highly identified in HUVECs compared with those in smooth muscle cells and cardiomyocytes. (B) Left, top 5 miRNA candidates in HUVECs. Right, flow cytometric analysis of candidate miRNA switches transfected in HUVECs. Blue dots represent BFP mRNA as a control. Red dots represent each miRNA switch. (C) Left, scatter plots comparing gene expression between primary hepatocytes and NHDF. Middle, top 5 miRNA candidates in primary hepatocytes. Right, flow cytometric analysis of candidate miRNA switches transfected in differentiated cells from hiPSCs induced using a hepatic differentiation protocol. (D) Representative flow cytometry plots of miR-375-switch in 585A1-derived cells at day 23. (E) Immunohistochemical analysis of INSULIN expression in miR-375-switch-sorted cells, N.F. cells and non-sorted cells in the other 2 experiments. The nuclei were stained with Hoechst. Scale bars, 100 μm.

Table S1, related to Figure 3

cTNT^{+} percentages in 4 hPSC lines after sorting by miRNA switches or antibodies.

		positive fraction					negative fraction					
		miR-1	miR-208a	miR-499a-5p	SIRPA+LIN-	VCAM1+	miR-1	miR-208a	miR-499a-5p	SIRPA+LIN-	VCAM1+	w/o sort
409B2	Ex1 (%)	96.8	96.3	93.4	87.2	88.2	11.0	15.8	22.8	15.5	36.8	51.3
	Ex2 (%)	94.6	96.1	94.3	92.6	93.6	13.7	17.5	19.9	10.1	35.7	34.2
	Ex3 (%)	94.4	94.7	96.7	82.4	86.1	16.9	19.5	29.6	18.9	41.9	40.6
	Ex4 (%)	96.0	96.9	90.6	72.8	85.4	15.8	13.0	25.4	23.4	28.8	27.9
	Average (%)	95.45	96.00	93.75	83.75	88.33	14.35	16.45	24.43	16.98	35.80	38.50
	SD	1.15	0.93	2.52	8.41	3.71	2.60	2.75	4.12	5.61	5.39	9.98

		positive fraction					negative fraction					
		miR-1	miR-208a	miR-499a-5p	SIRPA+LIN-	VCAM1+	miR-1	miR-208a	miR-499a-5p	SIRPA+LIN-	VCAM1+	w/o sort
947A2	Ex1 (%)	93.0	92.1	96.7	73.1	60.7	3.05	2.76	3.52	2.52	24.7	20.2
	Ex2 (%)	90.3	92.6	92.1	71.0	70.2	2.67	2.68	4.66	1.58	21.4	25.2
	Ex3 (%)	95.5	96.9	97.3	71.9	59.8	6.69	4.97	6.79	5.40	15.1	22.7
	Average (%)	92.93	93.87	95.37	72.00	63.57	4.14	3.47	4.99	3.17	20.40	22.70
	SD	2.60	2.64	2.84	1.05	5.76	2.22	1.30	1.66	1.99	4.88	2.50

		positive fraction					negative fraction					
		miR-1	miR-208a	miR-499a-5p	SIRPA+LIN-	VCAM1+	miR-1	miR-208a	miR-499a-5p	SIRPA+LIN-	VCAM1+	w/o sort
606A1	Ex1 (%)	95.6	94.7	97.2	81.3	84.7	4.86	8.98	11.2	15.4	20.1	41.6
	Ex2 (%)	96.9	96.3	97.0	82.5	86.5	3.16	3.13	18.6	9.02	35.8	46.5
	Ex3 (%)	94.2	97.1	94.7	78.9	80.5	15.9	12.0	27.2	9.80	38.5	49.7
	Average (%)	95.57	96.03	96.30	80.90	83.90	7.97	8.04	18.99	11.41	31.47	45.93
	SD	1.35	1.22	1.39	1.83	3.08	6.92	4.51	8.01	3.48	9.94	4.08

		positive fraction					negative fraction					
		miR-1	miR-208a	miR-499a-5p	SIRPA+LIN-	VCAM1+	miR-1	miR-208a	miR-499a-5p	SIRPA+LIN-	VCAM1+	w/o sort
KhES1	Ex1 (%)	95.3	96.2	94.9	85.6	79.6	7.81	6.28	30.6	22.8	28.7	39.4
	Ex2 (%)	95.9	96.1	97.1	70.1	60.3	15.8	4.41	24.5	10.2	20.8	44.8
	Ex3 (%)	94.3	93.6	92.1	74.1	83.5	10.1	11.8	21.4	4.88	11.1	31.4
	Average (%)	95.17	95.30	94.70	76.60	74.47	11.24	7.50	25.51	12.63	20.20	38.53
	SD	0.81	1.47	2.51	8.05	12.42	4.11	3.84	4.66	9.20	8.82	6.74

Table S2, related to Experimental Procedures Primer list.

PCR primers

Primer name	sequence (5' to 3')
FwdMCS	GGGATCCCATGGTGTCGACCTGCAGCATATGAGCTCCTGAATTCGCCCTATAGTGAGTCG
RevMCS	GGGAGATCTCATATGCATCTCGAGTGATAGTCTAGACAAGCTTGAGTATTCTATAGTGTCACC
CFwdtagBFP	GCCACCATGGGATCCAGCGAGCTGATTAAGGAGAAC
CRevtagBFP	ACTCGAGATCTGTGCCCCAGTTTGCTAG
CFwdEGFP	GAACCATGGGATCCGTGAGCAAGGGCGAGG
CRevEGFP	TATGAGATCTCTTGTACAGCTCGTCCATG
T7FwdA	GCTAATACGACTCACTATAGGTCAGATCCGCTAGGATC
Rev5UTR	CATGGTGGCGACCGGTGTCTTATATTTCTTCTTACTC
T7FwdG3C	CAGTGAATTGTAATACGACTCACTATAGGGC
temp5UTR	CAGTGAATTGTAATACGACTCACTATAGGGCGAATTAAGAGAGAAAAGAAGAGTAAGAAGAAATATAAGACACCGGTCGCCACCATG
Fwd3UTR	TCTAGACCTTCTGCGGGGC
Rev3UTR	TTTTTTTTTTTTTTTTTTTTCCTACTCAGGCTTTATTCAAAGACCAAG
temp3UTR	TCTAGACCTTCTGCGGGGCTTGCCTTCTGGCCATGCCCTTCTTCTCTCCCTTGCACCTGTACCTCTTGGTCTTTGAATAAAGCCTGA GTAGG
FwdtagBFP	CACCGGTCGCCACCATGGGATCCAGCGAG
FwdEGFP	CACCGGTCGCCACCATGGGATCCGTGAGCAAGGGC
RevORF	GCCCCGCAGAAGGTCTAGACTATCACTCGAGATGCATATGAGATC
FwdhdKRed	CACCGGTCGCCACCATGGTGAGCGTGATCGCCAAG
RevNPhdKRed	GCCCCGCAGAAGGTCTAGACTATTACTTTTTATCCTTTTCCTTTTTACTCTTCTTC
FwdBlastcidin	CACCGGTCGCCACCATGGCCAAGCCTTTGTC
RevBlastcidin	GCCCCGCAGAAGGTCTAGATTAGCCCTCCCACACATAACCAG
FwdPuromycin	CACCGGTCGCCACCATGACCGAGTACAAGCCCACG
RevPuromycin	GCCCCGCAGAAGGTCTAGATCAGGCACCGGGCTTGC
FwdORF	CACCGGTCGCCACCATG
RevBimEL	GCCCCGCAGAAGGTCTAGAATCAATGCATTCTCCACACCAG
Rev120A	TTTTTTTTTTTTTTTTTTTTTTTTTTTTTTTTTTTTTTTTTTTTTTTTTTTTTTTTTTTTTTTTTTTTTTTTTTTTTTTTTTTTTTT TTTTTTTTTTTTTTTTTTTTTTTTTTTTTTTTTCCTACTCAGGCTTTATTCA
T7FwdB	GCTAATACGACTCACTATAGGTTCCTTAATCGCGGATCC

Fragments inserted into plasmids

Oligo DNA name	sequence (5' to 3')
5Tmi21_Afwd	GATCCTCAACATCAGTCTGATAAGCTAAGATCTA

5Tmi21_Arev	CCGGTAGATCTTAGCTTATCAGACTGATGTTGAG
5Tmi17_5_Afwd	GATCCCTACCTGCACTGTAAGCACTTTGAGATCTA
5Tmi17_5_Arev	CCGGTAGATCTCAAAGTGCTTACAGTGCAGGTAGG

Template oligo DNAs for 5’ and 3’ UTRs

Oligo DNA name	sequence (5' to 3')
3UTRtemp_4xT21-5p	CCTACTCAGGCTTTATTCACGCGGCCGCGTAGCTTATCAGACTGATGTTGAGTAGCTTATCAGACTGATGTTGAGTAGCTTATCAGA CTGATGTTGAGTAGCTTATCAGACTGATGTTGACAGCTCGTCGCCCCGCAGAAGGTCTAGA
3UTRtemp_4xT17-5p	CCTACTCAGGCTTTATTCACGCGGCCGCCAAAGTGCTTACAGTGCAGGTAGCAAAGTGCTTACAGTGCAGGTAGCAAAGTGCTTACA GTGCAGGTAGCAAAGTGCTTACAGTGCAGGTAGCAGCTCGTCGCCCCGCAGAAGGTCTAGA
5UTRtemp_let-7e-5p	CGACTCACTATAGGTTCCGCGATCGCGGATCCAACTATACAACCTCCTACCTCAAGATCACACCGGTCGCCACCATG
5UTRtemp_T1	CGACTCACTATAGGTTCCGCGATCGCGGATCCATACATACTTCTTTACATTCCAAGATCACACCGGTCGCCACCATG
5UTRtemp_T22-5p	CGACTCACTATAGGTTCCGCGATCGCGGATCCTAAAGCTTGCCACTGAAGAACTAGATCACACCGGTCGCCACCATG
5UTRtemp_T133a-3p	CGACTCACTATAGGTTCCGCGATCGCGGATCCCAGCTGGTTGAAGGGGACCAAAAGATCACACCGGTCGCCACCATG
5UTRtemp_T133b	CGACTCACTATAGGTTCCGCGATCGCGGATCCTAGCTGGTTGAAGGGGACCAAAAGATCACACCGGTCGCCACCATG
5UTRtemp_T143-3p	CGACTCACTATAGGTTCCGCGATCGCGGATCCGAGCTACAGTGCTTCATCTCAAGATCAACACCGGTCGCCACCATG
5UTRtemp_T145-3p	CGACTCACTATAGGTTCCGCGATCGCGGATCCAGAACAGTATTTCCAGGAATCCAGATCACACCGGTCGCCACCATG
5UTRtemp_T208a-3p	CGACTCACTATAGGTTCCGCGATCGCGGATCCACAAGCTTTTTGCTCGTCTTATAGATCACACCGGTCGCCACCATG
5UTRtemp_T490-5p	CGACTCACTATAGGTTCCGCGATCGCGGATCCACCCACCTGGAGATCCATGGAGATCAAACACCGGTCGCCACCATG
5UTRtemp_T490-3p	CGACTCACTATAGGTTCCGCGATCGCGGATCCCAGCATGGAGTCCTCCAGGTTGAGATCACACCGGTCGCCACCATG
5UTRtemp_T499a-5p	CGACTCACTATAGGTTCCGCGATCGCGGATCCAAACATCACTGCAAGTCTTAAAGATCAACACCGGTCGCCACCATG
5UTRtemp_T1271-5p	CGACTCACTATAGGTTCCGCGATCGCGGATCCTGAGTGCTTGCTAGGTGCCAAGAGATCACACCGGTCGCCACCATG
5UTRtemp_T3907	CGACTCACTATAGGTTCCGCGATCGCGGATCCTGTGAGCCAGCCTGGAGCACCTAGATCACACCGGTCGCCACCATG
5UTRtemp_T4324	CGACTCACTATAGGTTCCGCGATCGCGGATCCTTAAGGTTAGGGTCTCAGGGAGATCAAACACCGGTCGCCACCATG
5UTRtemp_T10b-5p	CGACTCACTATAGGTTCCGCGATCGCGGATCCCACAAATTCGGTTCTACAGGGTAAGATCCACCGGTCGCCACCATG
5UTRtemp_T196b-5p	CGACTCACTATAGGTTCCGCGATCGCGGATCCCCCAACAACAGGAAACTACCTAAGATCACACCGGTCGCCACCATG
5UTRtemp_T126a-5p atog	CGACTCACTATAGGTTCCGCGATCGCGGATCCCGCGTACCAAAAGTAATAGTGAGATCAACACCGGTCGCCACCATG
5UTRtemp_T216a-5p	CGACTCACTATAGGTTCCGCGATCGCGGATCCTCACAGTTGCCAGCTGAGATTAAGATCACACCGGTCGCCACCATG
5UTRtemp_T126-3p	CGACTCACTATAGGTTCCGCGATCGCGGATCCCGCATTATTACTCACGGTACGAAGATCACACCGGTCGCCACCATG
5UTRtemp_T122-3p	CGACTCACTATAGGTTCCGCGATCGCGGATCCATATTTAGTGTGATAATGGCGTTAGATCCACCGGTCGCCACCATG
5UTRtemp_T122-5p	CGACTCACTATAGGTTCCGCGATCGCGGATCCCAAACACCATTGTCACACTCCAAGATCACACCGGTCGCCACCATG
5UTRtemp_T192-5p	CGACTCACTATAGGTTCCGCGATCGCGGATCCGGCTGTCAATTCATAGGTCAGAGATCAACACCGGTCGCCACCATG
5UTRtemp_T194-5p	CGACTCACTATAGGTTCCGCGATCGCGGATCCTCCACATGGAGTTGCTGTTACAAGATCACACCGGTCGCCACCATG
5UTRtemp_T215	CGACTCACTATAGGTTCCGCGATCGCGGATCCGTCTGTCAATTCATAGGTCATAGATCAACACCGGTCGCCACCATG
5UTRtemp_T24-3p	CGACTCACTATAGGTTCCGCGATCGCGGATCCCTGTTCCTGCTGAACTGAGCCAAGATCACACCGGTCGCCACCATG

5UTRtemp_T141-3p	CGACTCACTATAGGTTCCGCGATCGCGGATCCCCATCTTTACCAGACAGTGTTAAGATCACACCGGTCGCCACCATG
5UTRtemp_T200a-3p	CGACTCACTATAGGTTCCGCGATCGCGGATCCACATCGTTACCAGACAGTGTTAAGATCACACCGGTCGCCACCATG
5UTRtemp_T200b-3p	CGACTCACTATAGGTTCCGCGATCGCGGATCCTCATCATTACCAGGCAGTATTAAGATCACACCGGTCGCCACCATG
5UTRtemp_T200c-3p	CGACTCACTATAGGTTCCGCGATCGCGGATCCTCCATCATTACCCGGCAGTATTAAGATCCACCGGTCGCCACCATG
5UTRtemp_T331-3p	CGACTCACTATAGGTTCCGCGATCGCGGATCCTTCTAGGATAGGCCCAGGGGCAGATCAACACCGGTCGCCACCATG
5UTRtemp_T362-3p	CGACTCACTATAGGTTCCGCGATCGCGGATCCTGAATCCTTGAATAGGTGTGTTAGATCACACCGGTCGCCACCATG
5UTRtemp_T375	CGACTCACTATAGGTTCCGCGATCGCGGATCCTCACGCGAGCCGAACGAACAAAAGATCACACCGGTCGCCACCATG

Table S3, related to Experimental Procedures The PCR reaction conditions.

UTR

PCR product	Forward Primer	Reverse Primer	Template	Type of Template
control 5' UTR	T7FwdG3C	Rev5UTR	temp5UTR	oligoDNA
control 3' UTR	Fwd3UTR	Rev3UTR	temp3UTR	oligoDNA
5' UTR with miRNA target site	T7FwdA	Rev5UTR	T21-5p-ECFP (this study) or T17-5p-ECFP (this study)	plasmid

Protein-coding region

PCR product	Forward Primer	Reverse Primer	Template
tagBFP	FwdtagBFP	RevORF	pAM-tagBFP (this study)
EGFP	FwdEGFP	RevORF	pAM-EGFP (this study)
hdKeima-Red	FwdhdKRed	RevNPhdKRed	pNP-hdKeima-Red (Amargaam)
Blastcidin	FwdBlastcidin	RevBlastcidin	pLenti6/Ubc/V5-DEST (Life Technologies)
Puromycin	FwdPuromycin	RevPuromycin	pPyCAG-Nanog-IP (Addgene plasmid 13838)
BimEL	FwdORF	RevBimEL	pcDNA3.1-HsBimEL (Saito et al., 2011)

IVT template

PCR product	Forward Primer	5' UTR	(Protein-coding region)	3' UTR	Reverse Primer
control mRNA	T7FwdG3C	control 5' UTR		control 3' UTR	Rev120A
miRNA target site in the 5' UTR (PCR)	T7FwdA	5' UTR with miRNA target site		control 3' UTR	Rev120A
miRNA target site in the 5' UTR (oligo-DNA)	T7FwdB	oligo-DNA (5UTRtemp_Txxx)		control 3' UTR	Rev120A
miRNA target site in the 3' UTR	T7FwdG3C	control 5' UTR		Oligo-DNA (3UTRtemp_4xTxxx)	Rev120A

Table S4, related to Experimental Procedures List of Taqman probes.

	Assay ID
GAPDH	Hs99999905_m1
TNNT2	Hs00943911_m1
MYL2	Hs00166405_m1
MYL7	Hs00221909_m1
MYH6	Hs01101425_m1
NKX2.5	Hs00231763_m1
TBX5	Hs01052566_m1
MYH7	Hs01110632_m1
PECAM1	Hs00169777_m1
THY1	Hs00264235_s1
PDGFR-β	Hs01019589_m1
EGFP	Mr04329676_mr
RNU6B	001093
hsa-miR-1	002222
hsa-miR-208a	000511
hsa-miR-499a-5p	001352

Supplementary methods

Cell culture and differentiation

hPSCs were maintained in primate ES cell medium (ReproCELL) supplemented with 4 ng/mL of human recombinant basic fibroblast growth factor (bFGF) (Wako) on SNL feeders (Fujioka et al., 2004; Ohnuki et al., 2009; Takahashi et al., 2007). To differentiate hPSCs into a cardiac lineage, we modified a previously described protocol (Dubois et al., 2011). In brief, embryoid bodies (EBs) were generated in a 6-well ultra-low attachment plate (Corning) with 1.5 ml/well StemPro-34 (Invitrogen) media containing 2 mM L-glutamine (Invitrogen), $4x10^{-4}$ M monothioglycerol (MTG), 50 µg/ml ascorbic acid (AA), 150 µg/ml transferrin, 0.5% penicillin/streptomycin (Invitrogen), 10 µM ROCK inhibitor (Y-27632) and 2 ng/ml BMP4. On day 1, 1.5 ml of medium [StemPro-34, 2 mM L-glutamine, $4x10^{-4}$ M monothioglycerol (MTG), 50 µg/ml ascorbic acid (AA), 150 µg/ml transferrin, 0.5% penicillin/streptomycin, bFGF (10 ng/ml, 5 ng/ml final), activin A (12 ng/ml, 6 ng/ml final) and BMP4 (18 ng/ml, 10 ng/ml final)] was added to each well. On day 4, the EBs were washed with Iscove's modified Dulbecco's media (IMDM; Invitrogen) and then cultured in StemPro-34 medium containing 2 mM L-glutamine, $4x10^{-4}$ M monothioglycerol (MTG), 50 µg/ml ascorbic acid (AA), 150 µg/ml transferrin, 10 ng/ml vascular endothelial growth factor (VEGF) and 1 µM IWP-3 (Stemgent) for 4 days. On day 8, the medium was changed to StemPro-34 medium containing 2 mM L-glutamine, $4x10^{-4}$ M monothioglycerol (MTG), 50 µg/ml ascorbic acid (AA), 150 µg/ml transferrin, 0.5% penicillin/streptomycin, 10 ng/ml VEGF and 5 ng/ml bFGF (I_3 medium) every two days. The EBs were cultured in a 5% CO_2, 5% O_2, 90% N_2 environment for the first 12 days and then transferred to a 5% CO_2, 95%

air environment for the remainder of the culture period.

To differentiate hiPSCs (the 201B6 cell line) into hepatocytes, we modified a previously described protocol (Kajiwara et al., 2012). In brief, single hiPSCs were seeded in Matrigel-coated culture plates with RPMI 1640 medium containing 1× B27 supplement, 100 ng/ml activin A, 10 μM Y-27632 and 1 μM CHIR99021. On day 1, Y-27632 was omitted from the above medium, and 0.5 mM NaB was added to the medium. On day 5, the medium was changed to knockout DMEM containing 20% knockout serum replacement (KSR), 1 mM L-glutamine, 1% nonessential amino acids, 0.1 mM 2-mercaptoethanol, 1% DMSO, 10 ng/ml FGF and 20 ng/ml BMP4 for 6 days. On day 11, the medium was changed to hepatocyte culture medium (Lonza) containing 20 ng/ml hepatocyte growth factor (HGF) and 20 ng/ml oncostatin M (OSM) for 7 days.

To differentiate hiPSCs (the 585A1 cell line) into INSULIN-producing cells, we modified a previously described protocol (Kunisada et al., 2012; Nakagawa et al., 2014). In brief, hiPSCs were cultured in RPMI 1640 medium containing 1× B27 supplement, 10 μM Y-27632 and 3 μM CHIR99021 for 24 h. The next day, the medium was changed to RPMI 1640 medium containing 1× B27 supplement, 100 ng/ml activin A and 1 μM CHIR99021 for 3 days. Next, the cells were cultured with Improved MEM Zinc Option medium containing 0.5× B27 supplement, 1 μM dorsomorphin, 2 μM retinoic acid, and 10 μM SB431542 for 6 days. Then, the medium was changed to Improved MEM Zinc Option medium containing 0.5× B27 supplement, 10 μM forskolin, 10 μM dexamethasone, 5 μM Alk5 inhibitor II and 10 mM nicotinamide for 8 days.

HUVECs were purchased (C2517A, Lonza) and cultured in EGM™-2 Endothelial

Cell Growth Medium-2 BulletKit (Lonza). Human aortic smooth muscle cells (AoSMCs) were purchased (CC-2571, Lonza) and cultured in SmGM™-2 Smooth Muscle Growth Medium-2 BulletKit (Lonza). Human hepatocytes were purchased (IVT-F00995-P, BioreclamationIVT) and cultured in *InVitro*GRO CP Medium (BioreclamationIVT) with *Torpedo* Antibiotic Mix (BioreclamationIVT). HeLa cells (ATCC) were cultured in Dulbecco's modified Eagle's medium (DMEM)-F12 containing 10% FBS and 1% antibiotic antimycotic solution (Sigma-Aldrich, St. Louis, MO, USA). 293FT cells (Invitrogen, Carlsbad, CA, USA) were grown in DMEM supplemented with 10% FBS, 2 mM L-glutamine (Invitrogen), 0.1 mM non-essential amino acids (Invitrogen), 1 mM sodium pyruvate (Sigma) and 0.5% penicillin-streptomycin (Invitrogen).

Transfection of miRNA switches

To purify cardiomyocytes and endothelial cells derived from hPSCs, EBs were treated with collagenase type I for 1-2 h and then treated with 0.25% trypsin/EDTA for 5-10 min. Next, 50% FBS/IMDM was added to the EBs to neutralize trypsin, and then the EBs were pipetted gently to dissociate the cells. After dissociation, the cells were centrifuged at 1000 rpm for 5 min and re-suspended in the I_3 medium. Then, the cells were seeded in a fibronectin (Sigma)-coated 24-well plate ($2x10^5$ cells/well) or 6-well plate ($1x10^6$ cells/well) and incubated for 2 days at 37 °C in 5% CO_2. Two days later, miRNA switches were transfected into cells using a Stemfect RNA transfection kit according to the manufacturer's protocol (Stemgent). In brief, for one well from the 24-well plate for miR-BFP-switch, 12.5 µl/tube Stemfect Transfection Buffer was added to two sterilized 1.5-ml tubes. In

the first tube, 1.0 µl of the Stemfect RNA Transfection Reagent was added to the buffer and mixed. In the second tube, 1.0 µl of 100 ng/µl miR-BFP-switch and 1.0 µl of 100 ng/µl EGFP mRNA were added to the buffer and mixed. The diluted transfection reagent solution was added to the diluted mRNA solution and mixed. The complex was incubated for 15 min at room temperature. Meanwhile, the culture medium was changed to 500 µl of fresh I_3 medium without antibiotics. After 15 min, the complex was added to the cells, and the plate was gently rocked and incubated for 4 h at 37 °C in 5% CO_2. After 4 h, the medium was aspirated, the well was washed once with IMDM, and 500 µl of fresh I_3 medium was added to the well.

For one well from the 6-well plate for miR-Bim-switch, 50 µl/tube Stemfect Transfection Buffer was added to two sterilized 1.5-ml tubes. In the first tube, 4.0 µl of the Stemfect RNA Transfection Reagent was added. In the second tube, 1.0, 1.5 or 2.0 µl of 100 ng/µl miR-Bim-switch and 2.0 µl of 100 ng/µl puromycin resistance mRNA were added. The solutions in the two tubes were mixed and incubated for 15 min at room temperature. Meanwhile, the culture medium was changed to 2 ml of fresh I_3 medium without antibiotics. After 15 min, the mixed solution was added to the cells, and the plate was gently rocked and incubated for 4 h at 37 °C in 5% CO_2. After 4 h, the medium was removed, the well was washed once with IMDM, and 2ml of fresh I_3 medium including 2 µg/ml puromycin was added to the cells.

To purify hepatocytes derived from hiPSCs, cells at day 16 or 17 were treated with Accumax for 20 min and pipetted gently to dissociate the cells. After dissociation, the cells were centrifuged at 1000 rpm for 5 min and re-suspended

in hepatocyte culture medium containing 20 ng/ml HGF and 20 ng/ml OSM. The cells were seeded in collagen I-coated 6-well plate (Corning) at $2x10^6$ cells/well and incubated for 1 day at 37 °C in 5% CO_2. The next day, miRNA switches were transfected into cells using a Stemfect RNA transfection kit as described above.

To purify INSULIN-producing cells derived from hiPSCs, miRNA switches were transfected into cells without reseeding at day 18. The transfection protocol was as described above.

Flow cytometry and cell sorting

To analyze HeLa and 293FT cells, we used an Accuri C6 flow cytometer (BD Biosciences). FL1 (530/30 nm) and FL2 (585/40 nm) filters were used in the analysis of cotransfection of 2 mRNAs: FL1 for EGFP and FL2 for hmKO2. At 24 h after transfection, the cells were detached from a dish, filtered through a mesh and then subjected to flow cytometry.

MYH6-EIP4 EBs were dissociated in the same way as for the transfection of miRNA switches and re-suspended in PBS with 2% FBS. The dissociated cells were analyzed and sorted using a FACSAria II cell sorter (BD Biosciences).

For the analysis and sorting of mRNA-transfected cells to purify cardiomyocytes and endothelial cells derived from hPSCs, on the day after transfection, the cells were treated with trypsin for 2-3 min and then neutralized by IMDM with 50% FBS. Then, the cells were centrifuged at 1000 rpm for 5 min and re-suspended in PBS with 2% FBS. Next, the cells were analyzed and sorted. For the analysis and sorting of mRNA-transfected cells to purify hepatocytes and

INSULIN-producing cells derived from hPSCs, on the day after transfection, the cells were treated with Accumax for 5-10 min, centrifuged at 1000 rpm for 5 min and re-suspended in PBS with 2% FBS. Then, the cells were analyzed and sorted.

For cell surface marker analysis, the cells were stained with anti- SIRPA–PE/Cy7 (BioLegend; 1:20), anti-CD31-PE (BD; 1:25), anti-CD49a-PE (BD; 1:10), anti-CD90-PE (BD; 1:10) and anti-CD140b-PE (BD; 1:10).

For detecting the cardiac isoform of troponin T (cTNT), the cells were fixed in 4% paraformaldehyde (PFA) in PBS and stained with anti-cardiac troponin T antibody (clone 13-11; Thermo; 1:200) in PBS with 2% FBS and 0.5% saponin (Sigma). APC goat anti-mouse Ig (BD Pharmingen; 1:100) was used as a secondary antibody. For detecting ALBUMIN and HNF4A, cells were fixed in 4% PFA in PBS, permeabilized with 0.1% Triton X-100 and stained with anti-ALBUMIN (Bethyl; 1:200) or anti-HNF4A (Santa Cruz; 1:200) antibody in PBS with 0.1% Triton X-100. Alexa Fluor 647 donkey anti-goat IgG (Invitrogen 1:500) was used as a secondary antibody.

Immunohistochemistry

For cTNT staining, the sorted cells were seeded in a fibronectin-coated 24-well plate ($2x10^5$ cells/well) and incubated for 2 days. Then, the cells were fixed in 4% PFA and stained with anti-cardiac cTNT antibody in PBS with 2% goat serum and 0.5% saponin (Sigma). Alexa Fluor 488 goat anti-mouse IgG (Invitrogen; 1:500) was used as a secondary antibody. The nuclei were stained with Hoechst (Invitrogen; 1:10000). Sample images were acquired using a Biorevo BZ-9000 microscope (Keyence).

For ALBUMIN staining, the sorted cells were seeded in a collagen I-coated 24-well plate and incubated for one day. Then, the cells were fixed in 4% PFA, blocked with PBS containing 5% donkey serum (Chemicon), 1% BSA and 0.1% Triton X-100 for 45 min and stained with anti-ALBUMIN antibody as described above. Alexa Fluor 488 donkey anti-goat IgG (Invitrogen; 1:500) was used as a secondary antibody. The nuclei were stained with Hoechst. Sample images were acquired using a Pulse-SIM BZ-X700 microscope (Keyence).

For INSULIN staining, the sorted cells were seeded in a Matrigel-coated 384-well plate and incubated for one day. The cells were fixed with 4% PFA, blocked with PBS containing 5% donkey serum and 0.4% Triton X-100 and stained with anti-INSULIN antibody (Dako; 1:200). Guinea pig-647 (Jackson ImmunoResearch) was used as a secondary antibody. The nuclei were stained with Hoechst. Sample images were acquired using a BZ-X700 microscope (Keyence). To quantify the $INSULIN^{+}$ cell ratios, the immunostained cells were analyzed by manual counting.

For the transplanted hearts, the excised heart specimens were fixed in 4% PFA overnight. The next day, the specimens were immersed in 15% sucrose solution for 3-4 h and then immersed in 30% sucrose solution overnight. The next day, the samples were embedded in O.C.T. compound (Sakura Finetek) to create frozen sections. The frozen sections were stained with anti-human nuclei (Millipore; 1:200), anti-cardiac cTNT (Thermo; 1:100), anti-cardiac Troponin I (Santa Cruz; 1:100) and anti-Connexin 43 (Sigma; 1:500) antibodies. Alexa Fluor 647 donkey anti-goat IgG (Invitrogen; 1:500) and Alexa Fluor 546 donkey anti-mouse IgG (Invitrogen; 1:500) were used as secondary antibodies. The nuclei were stained

with Hoechst (Invitrogen; 1:10000). Sample images were acquired using a BZ-X700 microscope (Keyence).

RNA extraction

Cells were lysed using QIAzol lysis reagent (Qiagen), and total RNA was purified using an miRNeasy Mini Kit (Qiagen) according to the manufacturer's protocol. The RNA concentration and purity were determined by measuring the A260/280 ratios using a Nanodrop (Thermo Scientific). For microarrays, confirmation of the RNA quality was performed using a 2100 Bioanalyzer (Agilent Technologies).

Transplantation

We used non-obese diabetic/severe combined immunodeficiency interleukin-2 receptor γ^{null} (NOD/Shi-scid Il2rg^{null}; NOG) mice for transplantation into hearts and immunodeficient (SCID) mice for transplantation into testes.

For transplantation into hearts, we prepared 1x10^6 purified cardiomyocytes derived from a luciferase reporter-expressing hiPSC line using miR-208a-Bim-switch. The cells were suspended in 20 µl of culture medium and injected into the left ventricular myocardium directly after left anterior descending (LAD) coronary ligation. In vivo imaging system (IVIS; PerkinElmer) data were regularly monitored by intraperitoneal injection of a luciferin substrate. The hearts (*n*=3) were removed at approximately 3 months following transplantation and excised for immunostaining.

For transplantation into the testes, we prepared 2x10^4 hiPSCs (line; 201B7), 2 x10^5 201B7-derived non-purified cells, 2x10^5 miR-1-switch-sorted

cardiomyocytes and miR-208a-Bim-purified cardiomyocytes. The prepared cells were suspended in 50 μl of culture medium and injected into two testes (25 μl/testis). Three months later, the mice were euthanized, and teratoma incidence was evaluated.

The animal experiments were performed in accordance with the Guidelines for Animal Experiments of Kyoto University.

Supplementary References

Dubois, N.C., Craft, A.M., Sharma, P., Elliott, D.A., Stanley, E.G., Elefanty, A.G., Gramolini, A., and Keller, G. (2011). SIRPA is a specific cell-surface marker for isolating cardiomyocytes derived from human pluripotent stem cells. Nat Biotechnol 29, 1011-1018.

Fujioka, T., Yasuchika, K., Nakamura, Y., Nakatsuji, N., and Suemori, H. (2004). A simple and efficient cryopreservation method for primate embryonic stem cells. Int J Dev Biol 48, 1149-1154.

Kajiwara, M., Aoi, T., Okita, K., Takahashi, R., Inoue, H., Takayama, N., Endo, H., Eto, K., Toguchida, J., Uemoto, S., et al. (2012). Donor-dependent variations in hepatic differentiation from human-induced pluripotent stem cells. Proc Natl Acad Sci U S A 109, 12538-12543.

Kunisada, Y., Tsubooka-Yamazoe, N., Shoji, M., and Hosoya, M. (2012). Small molecules induce efficient differentiation into insulin-producing cells from human induced pluripotent stem cells. Stem Cell Res 8, 274-284.

Nakagawa, M., Taniguchi, Y., Senda, S., Takizawa, N., Ichisaka, T., Asano, K., Morizane, A., Doi, D., Takahashi, J., Nishizawa, M., et al. (2014). A novel efficient feeder-free culture system for the derivation of human induced pluripotent stem cells. Sci Rep 4, 3594.

Ohnuki, M., Takahashi, K., and Yamanaka, S. (2009). Generation and characterization of human induced pluripotent stem cells. Curr Protoc Stem Cell Biol Chapter 4, Unit 4A 2.

Saito, H., Fujita, Y., Kashida, S., Hayashi, K., and Inoue, T. (2011). Synthetic human cell fate regulation by protein-driven RNA switches. Nat Commun 2, 160.

Takahashi, K., Tanabe, K., Ohnuki, M., Narita, M., Ichisaka, T., Tomoda, K., and Yamanaka, S. (2007). Induction of pluripotent stem cells from adult human fibroblasts by defined factors. Cell 131, 861-872.